CD5-NK1.1+ γδT Cells that Develop in a Bcl11b-Independent Manner Participate in Early Protection against Infection

畑野, 晋也

https://doi.org/10.15017/1931794

出版情報：九州大学, 2017, 博士（医学）, 課程博士
バージョン：

Article

Cell Reports

CD5⁻NK1.1⁺ γδ T Cells that Develop in a Bcl11b-Independent Manner Participate in Early Protection against Infection

Graphical Abstract

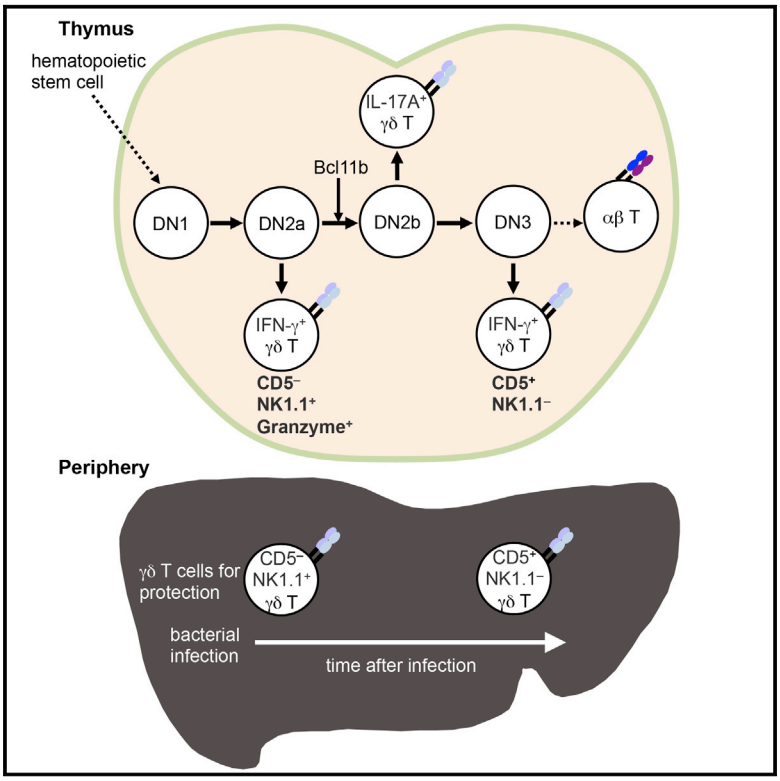

Authors

Shinya Hatano, Tesshin Murakami, Naoto Noguchi, Hisakata Yamada, Yasunobu Yoshikai

Correspondence

yoshikai@bioreg.kyushu-u.ac.jp

In Brief

Bcl11b is essential for transition from the DN2a to the DN2b stage in the thymus. Hatano et al. find that CD5⁻NK1.1⁺ γδ T cells develop from the DN2a stage in a Bcl11b-independent manner and participate in host defense at an early stage after bacterial infection in periphery.

Highlights

- CD5⁻NK1.1⁺ γδ T cells develop from DN2a thymocytes independently of Bcl11b
- CD5⁻NK1.1⁺ γδ T cells are IFN-γ⁺ Granzyme B⁺ and abundant in the liver of young mice
- CD5⁻NK1.1⁺ γδ T cells contribute to early protection against *Listeria* infection
- Appearance of γδ T cells in host defense resembles that in thymic development

Data and Software Availability

GSE89906

Hatano et al., 2017, Cell Reports *21*, 1191–1202
October 31, 2017
https://doi.org/10.1016/j.celrep.2017.10.007

Cell Reports
Article

CD5$^-$NK1.1$^+$ γδ T Cells that Develop in a Bcl11b-Independent Manner Participate in Early Protection against Infection

Shinya Hatano,[1] Tesshin Murakami,[1] Naoto Noguchi,[1] Hisakata Yamada,[1] and Yasunobu Yoshikai[1,2,*]
[1]Division of Host Defense, Medical Institute of Bioregulation, Kyushu University, Fukuoka 812-8582, Japan
[2]Lead Contact
*Correspondence: yoshikai@bioreg.kyushu-u.ac.jp
https://doi.org/10.1016/j.celrep.2017.10.007

SUMMARY

We recently found that a unique subset of innate-like γδ T cells develops from the DN2a stage of the fetal thymus independently of the zinc-finger transcription factor B cell leukemia/lymphoma 11b (Bcl11b). Herein, we characterize these Bcl11b-independent γδ T cells in the periphery as CD5$^-$NK1.1$^+$ and Granzyme B$^+$, and we show that they are capable of producing interferon (IFN)-γ upon T cell receptor stimulation without Ca^{2+} influx. In wild-type mice, these cells were sparse in lymphoid tissues but abundant in non-lymphoid tissues, such as the liver. Bcl11b-independent CD5$^-$NK1.1$^+$ γδ T cells appeared and contributed to early protection before Bcl11b-dependent CD5$^+$NK1.1$^-$ γδ T cells following *Listeria monocytogenes* infection, resembling their sequential appearance during development in the thymus.

INTRODUCTION

In the thymus, two types of T cells develop: γδ T cell receptor (TCR)-positive cells, which develop from the CD4$^-$CD8$^-$ double-negative (DN) stage (Hayday and Pennington, 2007; Petrie et al., 1992; Prinz et al., 2006), whereas cell populations that enter the CD4$^+$CD8$^+$ double-positive (DP) stage become αβ T cells (Yui and Rothenberg, 2014). Unlike conventional αβ T cells, which are exported from the thymus as naive cells and acquire effector functions upon encountering antigen in the periphery, murine γδ T cells are functionally committed to forming effector cells that produce inflammatory cytokines, such as interferon (IFN)-γ and interleukin (IL)-17, within the thymus, and they are disproportionately distributed within mucosal epithelia (Chien et al., 2014; Ribot et al., 2009; Shibata et al., 2008; Vantourout and Hayday, 2013). B cell leukemia/lymphoma 11B (Bcl11b) is a zinc-finger transcription factor (Avram et al., 2002; Satterwhite et al., 2001; Wakabayashi et al., 2003a) that is essential for transition from the early DN2a stage (CD117^{high} CD44$^+$ CD25$^+$) to the late DN2b stage (CD117^{intermediate} CD44$^+$ CD25$^+$) during the stepwise maturation from DN1 (CD117$^+$ CD44$^+$ CD25$^-$) to DN4 cells (CD117$^-$ CD44$^-$ CD25$^-$) (Avram and Califano, 2014; Ikawa et al., 2010; Li et al., 2010a; Liu et al., 2010; Wakabayashi et al., 2003b). Using germline Bcl11b knockout (KO) mice, we recently found that IL-17A$^+$ γδ T cells develop directly from DN2b-stage cells in a Bcl11b-dependent manner. In contrast, there are two subsets of IFN-γ$^+$ γδ T cells: one developing from DN2a-stage cells in a Bcl11b-independent manner and another from DN3-stage cells in a Bcl11b-dependent manner (Shibata et al., 2014).

The early γδ T cell response to infection with various microbial pathogens and tumor development suggests that a significant fraction of γδ T cells form the first-line host defense (Chien et al., 2014). It has been reported that the number of γδ T cells significantly increases at the early stage of primary infection with *Listeria monocytogenes* in mice (Ohga et al., 1990; Skeen and Ziegler, 1993). These γδ T cells produced Th1-type cytokines, particularly IFN-γ, and a study using mice depleted of γδ T cells by in vivo treatment with TCRγδ monoclonal antibody (mAb) revealed that γδ T cells play a protective role, at least during the early stages of bacterial infection (Hiromatsu et al., 1992). This hypothesis was strengthened by the findings of a study using TCRγ gene-targeted mice (Mombaerts et al., 1993). Among the innate-like γδ T cells in the fetal thymus committed to forming IFN-γ-producing effector cells, those programmed to develop at the earlier DN2 stage in a Bcl11b-independent manner seemed to be more primitive T cells of the innate immune system. The ontogenetic wave of γδ T cell development in the thymus suggests that Bcl11b-independent γδ T cells play a critical role in protecting against infections at the earlier stages after infection.

To test this hypothesis, we characterized the innate-like γδ T cells that developed from the DN2a stage in a Bcl11b-independent manner using Bcl11b conditionally deleted mice, in which T cell development was completely blocked before the DP stage. These studies showed that Bcl11b-independent γδ T cells are CD5$^-$ NK1.1$^+$ NKp46$^+$ NKG2D$^+$ CD244$^+$ Granzyme B$^+$ and capable of producing IFN-γ without Ca^{2+} influx upon TCR stimulation. In wild-type (WT) mice, CD5$^-$NK1.1$^+$ γδ T cells, which correspond to Bcl11b-independent γδ T cells, are sparse in lymphoid tissues but abundant in non-lymphoid tissues, such as the liver. Bcl11b-independent CD5$^-$NK1.1$^+$ γδ T cells appeared earlier than Bcl11b-dependent CD5$^+$NK1.1$^-$ γδ T cells, and they contributed to early protection following *L. monocytogenes* infection, resembling their sequential appearance during development in the thymus.

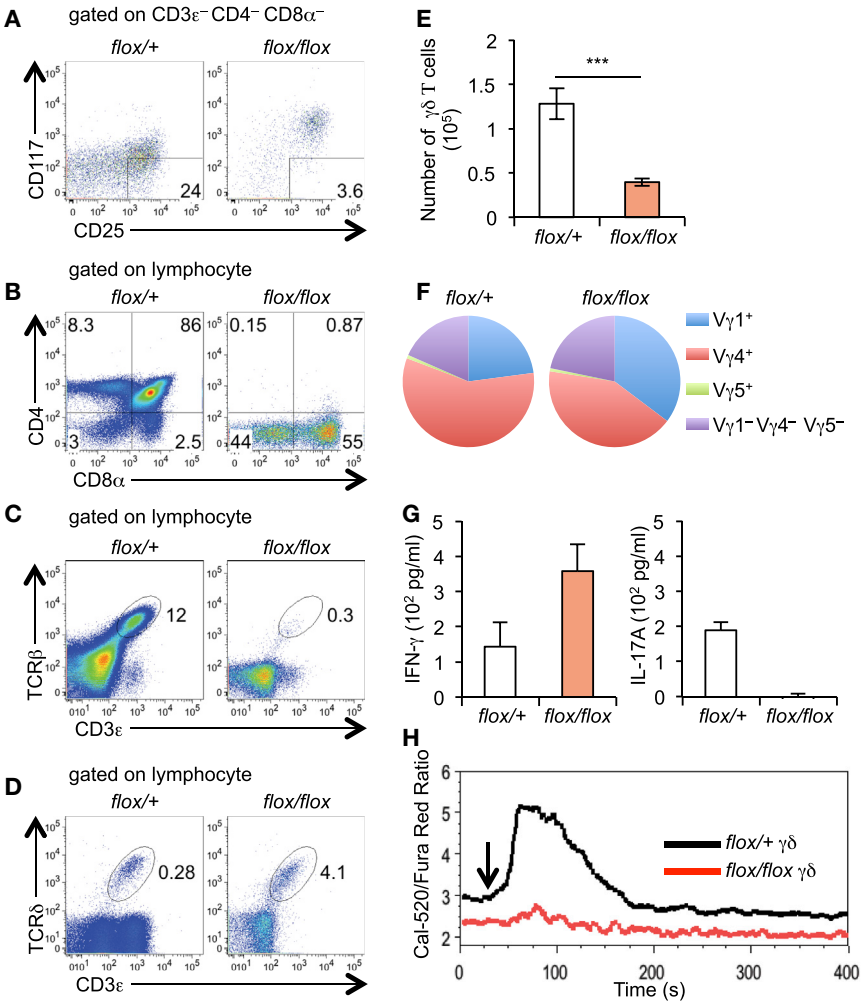

Figure 1. T Cell Development in the Thymus in the Absence of Bcl11b

(A) Representative dot plots are shown after gating on CD3ε⁻ CD4⁻ CD8α⁻ cells. Numbers indicate the percentages of DN3 (CD117⁻ CD25⁺) cells in the thymus from *flox*/+ and *flox/flox* mice (n = 3).

(B) Representative dot plots are shown after gating on lymphocytes. Numbers in the quadrants indicate the percentages of expression of CD4 and CD8α in lymphocytes of thymus from *flox*/+ and *flox/flox* mice (n = 3).

(C and D) Representative dot plots are shown after gating on lymphocytes. Numbers indicate the percentages of αβ T cells (C) and γδ T cells (D) in the thymus from *flox*/+ and *flox/flox* mice (n = 3).

(E) Bar graphs show the means ± SD of number of γδ T cells in the thymus from *flox*/+ and *flox/flox* mice (n = 3).

(F) Pie charts show the percentage of TCR Vγ repertoire of γδ T cells in the thymus from *flox*/+ and *flox/flox* mice (n = 3).

(G) Bar graphs show the means ± SD of production of IFN-γ and IL-17A of γδ T cells in the thymus from *flox*/+ and *flox/flox* mice after being stimulated with an anti-TCRδ mAb (n = 5). IFN-γ and IL-17A levels in 3-day cell culture supernatants were analyzed by ELISA.

(H) Intracellular Ca^{2+} mobilization in γδ T cells of thymus from *flox*/+ and *flox/flox* mice. Thymocytes were loaded with the Ca^{2+} dye Cal-520 and Fura-red. Cells were stimulated with biotinylated anti-CD3ε mAb followed by streptavidin cross-linking (downward arrow indicates when streptavidin was added). Results are the Ca^{2+} response to the gated population of γδ T cells.

Significant differences are shown (***p < 0.001, Student's t test). See also Figure S1.

RESULTS

Bcl11b-Independent γδ T Cells Function in the Thymus

Homozygous mutant Bcl11b KO mice developed severe neurological and other uncharacterized defects, and they died shortly after birth (Wakabayashi et al., 2003b). To characterize Bcl11b-independent γδ T cells after the neonatal stage, we generated mice in which Bcl11b was conditionally deleted by overexpression of the Cre recombinase under the control of the *Rag1* promoter (*CreRag1*;*Bcl11b*$^{flox/flox}$ mice, referred to hereafter as *flox/flox* mice). The *flox/flox* mice had a smaller body size compared with WT mice starting from around 7 weeks of age, and they died at 15 weeks as a result of severe inflammation. Therefore, we mainly examined healthy 3-week-old mice. T cell development in the thymus was completely blocked at the DN2 stage before transition to CD4$^+$ CD8$^+$ DP cells, resulting in the complete loss of CD4$^+$ CD8$^+$ DP cells in the thymus of *flox/flox* mice (Figures 1A and 1B). Thus, very few αβ T cells were detected in the thymus (Figure 1C), while appreciable levels of γδ T cells were detected in the thymus of *flox/flox* mice, although the absolute number of γδ T cells was significantly decreased compared with controls (*CreRag1*;*Bcl11b*$^{flox/+}$ mice, referred to hereafter as *flox*/+ mice) (Figures 1D and 1E).

γδ T cells expressing Vγ5, Vγ6, Vγ4, Vγ1/2, or Vγ7 (TCR nomenclature by Heilig and Tonegawa [1986]) develop sequentially in the fetal thymus from around embryonic day (E)12 (Havran and Allison, 1988). The variable (V) repertoire of γδ T cells in the thymus of 3-week-old mice was assessed by staining with anti-Vγ1, anti-Vγ4, or anti-Vγ5 mAb and RT-PCR. The γδ T cells in the thymus mainly consisted of Vγ1$^+$, Vγ4$^+$, and Vγ1$^-$ Vγ4$^-$ Vγ5$^-$ (presumably Vγ6$^+$, as assessed by RT-PCR) γδ T cells, but Vγ5$^+$ γδ T cells were rarely detected (Figures 1F and S1A). There were no remarkable differences in the Vγ repertoire of γδ T cells in the thymus of *flox/flox* mice and *flox*/+ mice. In agreement with previous findings of neonatal thymocytes in homozygous mutant Bcl11b KO mice (Shibata et al., 2014), IFN-γ production by γδ T cells was detected in *flox/flox* mice after stimulation via γδTCR, while IL-17A production was completely absent in *flox/flox* mice upon γδTCR stimulation (Figure 1G).

As Bcl11b is involved in various signaling pathways downstream of TCR, such as the pathway controlling calcium

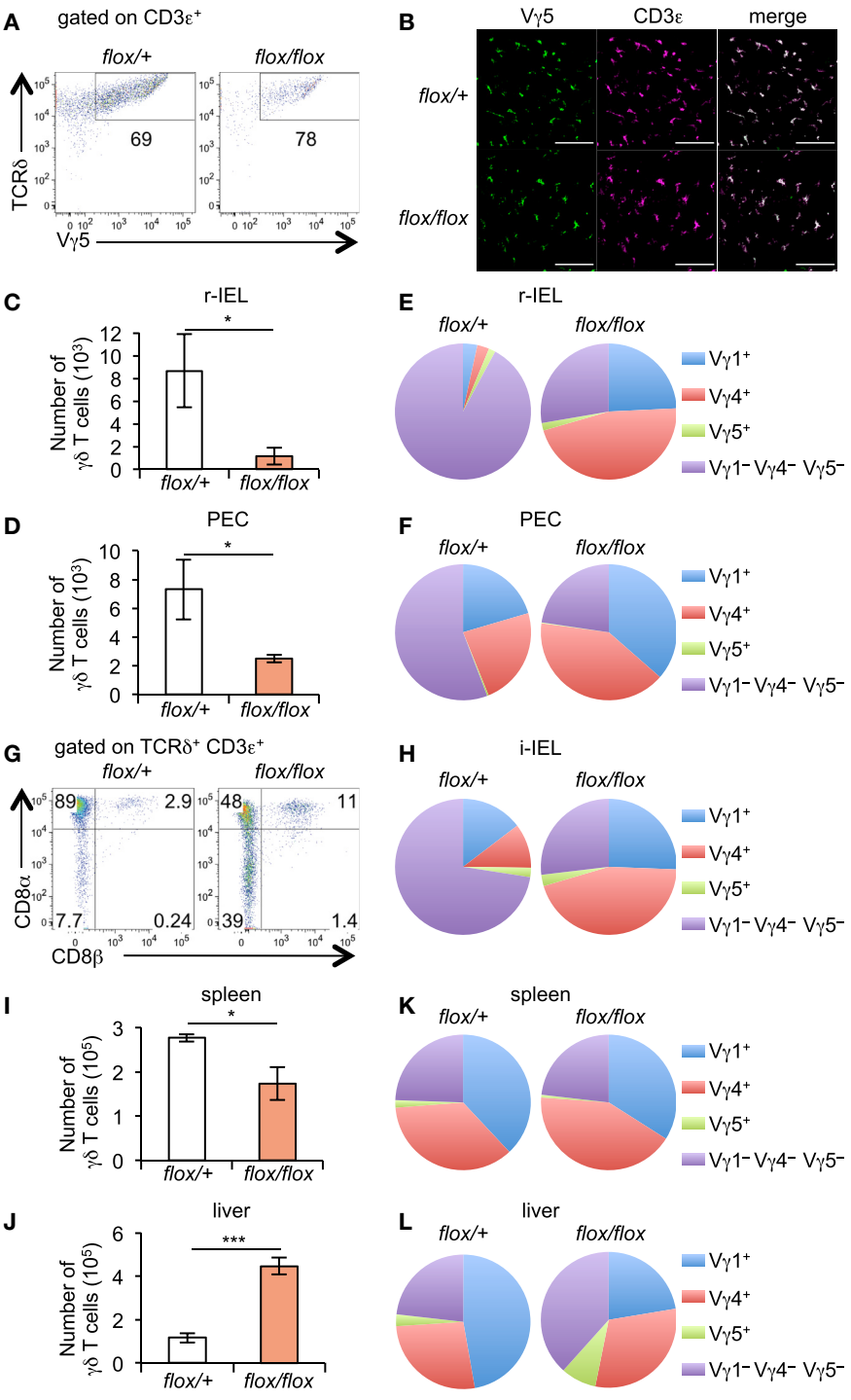

Figure 2. Tissue Distribution of Bcl11b-Independent γδ T Cells

(A) Representative dot plots are shown after gating on CD3ε+ cells. Numbers indicate the percentages of s-IELs in ears from *flox*/+ and *flox/flox* mice (n = 3).

(B) Paraformaldehyde-fixed epidermal sheets of ears from *flox*/+ and *flox/flox* mice were probed with anti-Vγ5 (green) and anti-CD3ε (magenta) mAb. Scale bars represent 100 μm.

(C and D) Bar graphs show the means ± SD of number of γδ T cells in r-IEL (C) and PEC (D) from *flox*/+ and *flox/flox* mice (n = 4).

(E and F) Pie charts show the percentage of TCR Vγ repertoire of γδ T cells in r-IEL (E) and PEC (F) from *flox*/+ and *flox/flox* mice (n = 4).

(G) Representative dot plots are shown after gating on TCRδ+ CD3ε+ cells. Numbers in the quadrants indicate the percentages of expression of CD8α and CD8β in γδ T cells of i-IEL from *flox*/+ and *flox/flox* mice (n = 3).

(H) Pie charts show the percentage of TCR Vγ repertoire of γδ T cells in i-IEL from *flox*/+ and *flox/flox* mice (n = 3).

(I and J) Bar graphs show the means ± SD of number of γδ T cells in spleen (I) and liver (J) from *flox*/+ and *flox/flox* mice (n = 3).

(K and L) Pie charts show the percentage of TCR Vγ repertoire of γδ T cells in spleen (K) and liver (L) from *flox*/+ and *flox/flox* mice (n = 3).

Significant differences are shown (*$p < 0.05$ and ***$p < 0.001$, Student's t test). See also Figure S1.

(Ca^{2+}) influx (Albu et al., 2007; Hirose et al., 2015; Inoue et al., 2006), we compared the intracellular Ca^{2+} ([Ca^{2+}]i) profile of γδ T cells in *flox/flox* and *flox*/+ mice upon γδTCR stimulation. The γδ T cells from *flox/flox* mice had an impaired Ca^{2+} response, whereas γδ T cells from *flox*/+ mice had a high initial (Ca^{2+})i spike, followed by a rapid decrease with few oscillations (Figure 1H). Thus, γδ T cells can produce IFN-γ without Ca^{2+} influx upon γδTCR stimulation in the absence of Bcl11b.

Bcl11b-Independent γδ T Cells Are Localized in Peripheral Tissues

γδ T cells preferentially migrate into mucosal epithelia (for example, of the skin, intestine, and uterus) as tissue-associated cells, and the proportion of γδ T cells depends on their TCR V repertoire and anatomical location (Hayday and Tigelaar, 2003). To determine the tissue distribution of Bcl11b-independent γδ T cells, we examined the presence of γδ T cells in peripheral tissues, including the skin, uterus, peritoneal cavity (PEC), and intestine of *flox/flox* mice. Vγ5+ γδ T cells, which are exclusively present in the skin intraepithelial lymphocyte (s-IEL) population (Asarnow et al., 1988; Bonneville et al., 1988), were equally detected in *flox/flox* and *flox*/+ mice (Figures 2A and 2B), whereas Vγ1− Vγ4− Vγ5− γδ T cells bearing a Vγ6+ chain, which are predominantly present in female reproductive organ IELs (r-IELs) (Itohara et al., 1990) and PEC (Mokuno et al., 2000), were reduced in the r-IELs and the PEC from *flox/flox* mice compared with *flox*/+ mice (Figures 2C–2F). In the small

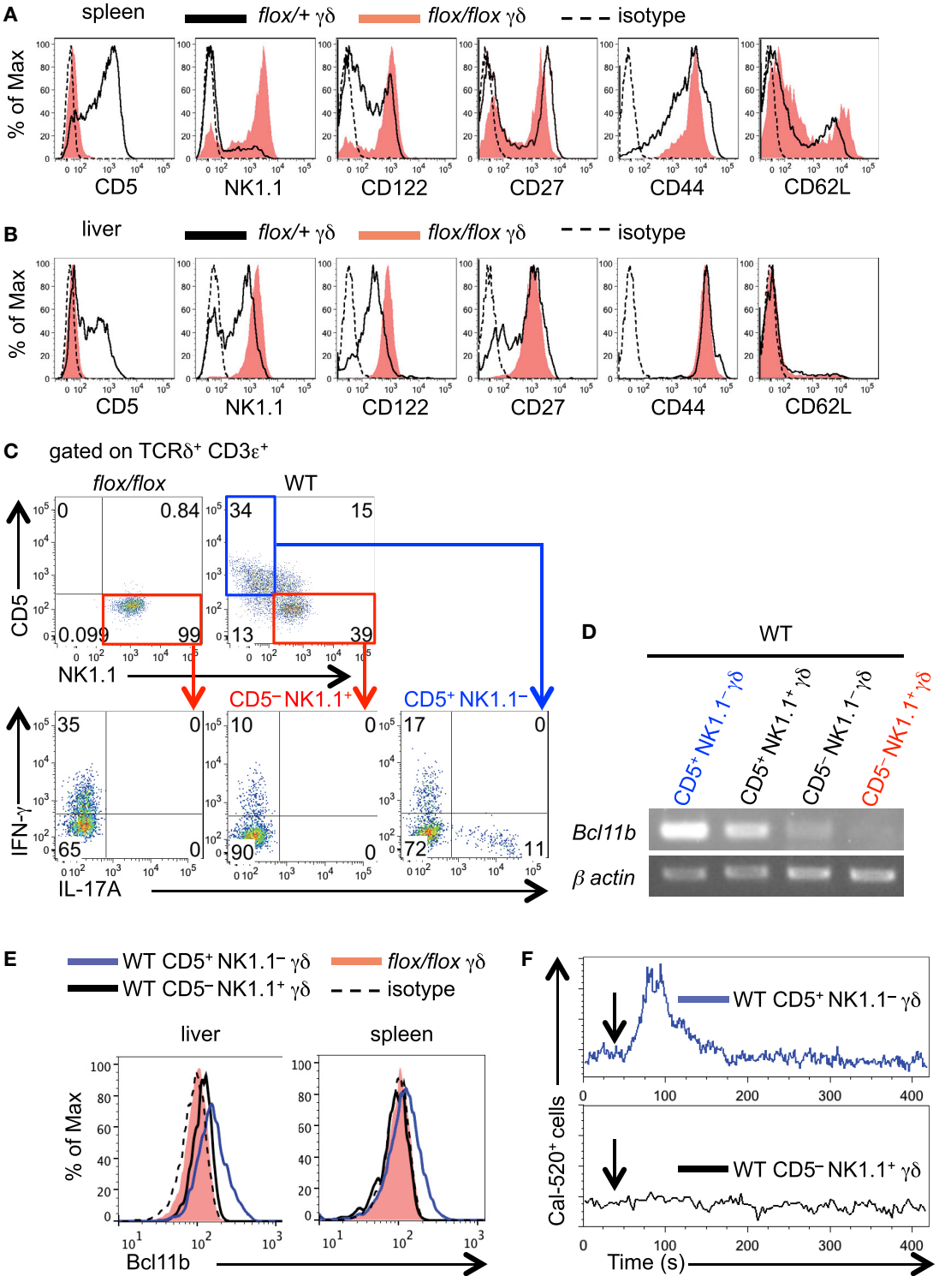

Figure 3. Surface Characteristics of Bcl11b-Independent γδ T Cells

(A and B) Histograms show expression of CD5, NK1.1, CD122, CD27, CD44, and CD62L on γδ T cells of the spleen (A) and liver (B) from *flox*/+ and *flox/flox* mice. Data are representative of 3 mice from each group.

(C) Upper dot plots are shown after gating on TCRδ+ CD3ε+ cells. Numbers in the quadrants indicate the percentages of expression of CD5 and NK1.1 in γδ T cells of liver from *flox/flox* and WT mice. Lower dot plots are shown after gating on CD5−NK1.1+ and CD5+NK1.1− γδ T cells. Numbers in the quadrants indicate the percentages of expression of intracellular IFN-γ and IL-17A after PMA/ionomycin stimulation. Data are representative of 3 mice from each group.

(legend continued on next page)

intestine, most γδ intestinal IELs (i-IELs) had a CD8αα phenotype in *flox*/+ mice, as reported previously (Goodman and Lefrancois, 1989), whereas CD8αα γδ i-IELs were selectively reduced in *flox/flox* mice (Figure 2G). Vγ1$^-$ Vγ4$^-$ Vγ5$^-$ γδ i-IELs bearing a Vγ7$^+$ chain, as assessed by RT-PCR and uniquely present in i-IELs (Goodman and Lefrancois, 1989), were decreased, whereas Vγ1$^+$ or Vγ4$^+$ γδ i-IELs were increased in *flox/flox* mice compared with *flox*/+ mice (Figures 2H and S1B). We compared the Vγ repertoire of γδ T cells in the spleen and liver of *flox/flox* and *flox*/+ mice. Although the absolute number of γδ T cells was significantly reduced in the spleen of *flox/flox* mice, there were no obvious differences in the Vγ repertoire of γδ T cells between *flox/flox* mice and *flox*/+ mice (Figures 2I, 2K, and S1C). In the liver, the absolute number of γδ T cells was increased in *flox/flox* mice, accompanied by increased percentages of Vγ1$^-$ Vγ4$^-$ Vγ5$^-$ γδ T cells bearing a Vγ6 chain and Vγ5$^+$ γδ T cells (Figures 2J, 2L, and S1D).

Bcl11b-Independent γδ T Cells Have a CD5$^-$ NK1.1$^+$ NKp46$^+$ NKG2D$^+$ Granzyme B$^+$ CD244$^+$ Phenotype

We next characterized the cell surface phenotype of Bcl11b-independent γδ T cells in the spleen and liver of *flox/flox* mice. Naive γδ T cells in *flox/flox* mice were characterized as CD5$^-$ NK1.1$^+$ CD122$^+$ CD27$^+$ CD44$^+$, while those in *flox*/+ mice contained heterogenous cell subsets based on the expression levels of CD5, NK1.1, and CD122 (Figures 3A and 3B). CD5$^-$NK1.1$^+$ expression was unchanged, but CD122 expression was decreased in IFN-γ$^+$ γδ T cells from *flox/flox* mice activated with phorbol myristate acetate (PMA) and ionomycin (Figures S2A and S2B). Taken together, γδ T cells from *flox/flox* mice are phenotypically distinguishable in *flox*/+ mice by differences in the expression of CD5 and NK1.1.

To confirm the presence of Bcl11b-independent γδ T cells in the periphery of WT mice, we examined cytokine production and *Bcl11b* expression of CD5$^-$NK1.1$^+$ γδ T cells in WT mice. In the liver of *flox/flox* mice, these cells produced IFN-γ, but not IL-17A, upon PMA/ionomycin stimulation. In WT mice, CD5$^-$NK1.1$^+$ γδ T cells produced IFN-γ, but not IL-17A, upon PMA/ionomycin stimulation, whereas CD5$^+$NK1.1$^-$ γδ T cells produced either IFN-γ or IL-17A upon stimulation (Figure 3C). In WT mice, a high level of *Bcl11b* expression at both the mRNA and protein levels was detected in CD5$^+$NK1.1$^-$, but not in CD5$^-$NK1.1$^+$, γδ T cells (Figures 3D and 3E). Thus, we confirmed that CD5$^-$NK1.1$^+$ γδ T cells (corresponding to Bcl11b-independent γδ T cells in *flox/flox* mice) are present in WT mice. We further compared the (Ca^{2+})i profile between CD5$^+$NK1.1$^-$ and CD5$^-$NK1.1$^+$ γδ T cells from WT mice upon γδ TCR stimulation. CD5$^-$NK1.1$^+$ γδ T cells had an impaired Ca^{2+} response, whereas CD5$^+$NK1.1$^-$ γδ T cells had a high initial (Ca^{2+})i spike, followed by a rapid decrease with few oscillations (Figure 3F). Thus, CD5$^-$NK1.1$^+$ γδ T cells were impaired in Ca^{2+} influx upon γδTCR stimulation.

We next analyzed global gene expression by comparing the transcriptome profiles of whole γδ T cells from the liver of *flox/flox* mice, in which more than 99% were CD5$^-$NK1.1$^+$, and prototypical Bcl11b-independent γδ T cells (CD5$^-$NK1.1$^+$ γδ T cells) and a prototypical Bcl11b-dependent γδ T cell subset (CD5$^+$NK1.1$^-$ γδ T cells) sorted from the liver of WT mice. These data showed that 1,345 probe sets were differentially expressed in CD5$^-$NK1.1$^+$ γδ T cells from WT mice compared with CD5$^+$NK1.1$^-$ γδ T cells from WT mice. Genes overexpressed in CD5$^-$NK1.1$^+$ γδ T cells from *flox/flox* or WT mice included *Gzmb*, *Prf1*, *Cd7*, *Clec7a*, *Ccl3*, *Ccl4*, and *Ccl5*. Levels of *Il7r*, *Il18r1*, *Il23r*, and *Rorc* expression were lower in the CD5$^-$NK1.1$^+$ γδ T cells than in the Bcl11b-dependent CD5$^+$NK1.1$^-$ γδ T cells (Figure 4A). For further analysis, we stained CD5$^-$NK1.1$^+$ and CD5$^+$NK1.1$^-$ γδ T cells from WT mice and γδ T cells from *flox/flox* mice with the corresponding mAbs. Consistent with the gene expression data, γδ T cells from *flox/flox* mice and CD5$^-$NK1.1$^+$ γδ T cells from WT mice expressed higher levels of NKp46, NKG2D, CD244, and Granzyme B and lower level of CD127 protein compared with CD5$^+$NK1.1$^-$ γδ T cells (Figure 4B). Although the mean fluorescence intensity (MFI) of each antigen was not identical (Figure 4B), CD5$^-$NK1.1$^+$ γδ T cells from WT mice were phenotypically similar to γδ T cells from *flox/flox* mice.

Bcl11b-Independent γδ T Cells Are Abundant in the Liver of WT Mice

We next examined the effect of location and age on the number of CD5$^-$NK1.1$^+$ γδ T cells in various organs of 3-week-old WT mice. CD5$^-$NK1.1$^+$ γδ T cells were relatively abundant in the liver (Figures 5A–5C). The numbers and populations of CD5$^-$NK1.1$^+$ γδ T cells in the liver increased to a peak at 21 days and then decreased (Figures 5D–5F). Thus, CD5$^-$NK1.1$^+$ γδ T cells were relatively abundant in the liver of young mice. In other non-lymphoid organs, such as lung and gut, appreciable numbers of CD5$^-$NK1.1$^+$ γδ T cells were detected in young mice (Figure S3).

To determine whether Bcl11b-independent CD5$^-$NK1.1$^+$ γδ T cells develop in the thymus only during fetal stages or not, we examined the development of CD5$^-$NK1.1$^+$ γδ T cells in lethally irradiated mice reconstituted with bone marrow (BM) or fetal liver (FL) cells (Figure S4A). CD5$^-$NK1.1$^+$ γδ T cells were detected in the liver of either of these reconstituted mice (Figure S4B). These γδ T cells expressed CD244 and NKG2D, but no CD127 or Bcl11b, similar to those in *flox/flox* mice

(D) CD5$^+$NK1.1$^-$, CD5$^+$NK1.1$^+$, CD5$^-$NK1.1$^-$, and CD5$^-$NK1.1$^+$ γδ T cells were sorted from the liver of WT mice, and *Bcl11b* expression was analyzed by RT-PCR.

(E) Histograms show expression of intracellular Bcl11b in CD5$^+$NK1.1$^-$ γδ T cells, CD5$^-$NK1.1$^+$ γδ T cells from WT mice, and γδ T cells from *flox/flox* mice in liver and spleen.

(F) Intracellular Ca^{2+} mobilization in CD5$^+$NK1.1$^-$ and CD5$^-$NK1.1$^+$ γδ T cells of spleen from WT mice. Cells were loaded with the Ca^{2+} dye Cal-520 and stimulated with biotinylated anti-CD3ε mAb followed by streptavidin crosslinking (downward arrow indicates when streptavidin was added). Results are the Ca^{2+} response to the gated population of CD5$^+$NK1.1$^-$ and CD5$^-$NK1.1$^+$ γδ T cells.

See also Figure S2.

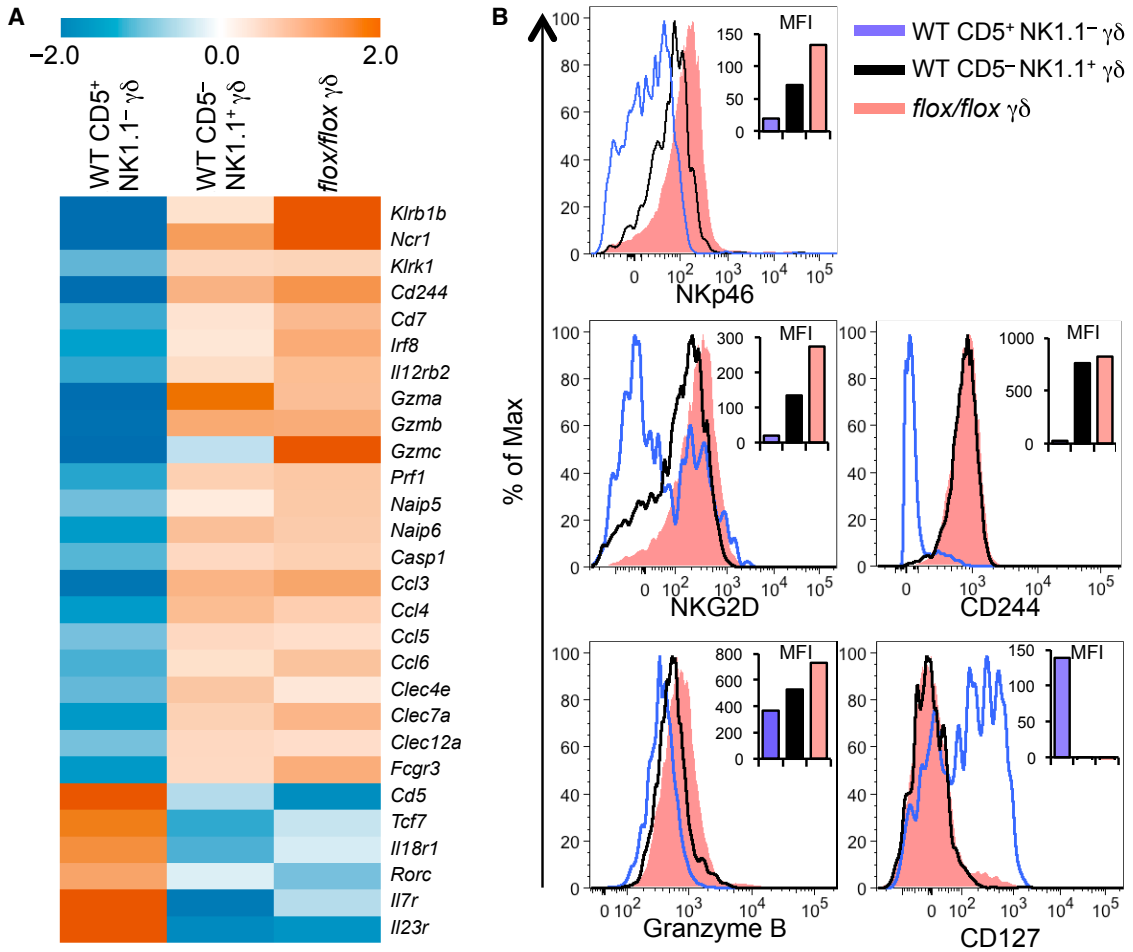

Figure 4. Microarray Analysis of Gene Expression in CD5$^-$NK1.1$^+$ γδ T Cells

(A) Microarray analysis of gene expression in CD5$^+$NK1.1$^-$ γδ T cells, CD5$^-$NK1.1$^+$ γδ T cells from the liver of WT mice, and γδ T cells from the liver of *flox/flox* mice (1 replicate of cells from 20 mice per sample). Color indicates the distance from the mean for each probe intensity (log_2 transformed).

(B) Histograms show expression of NKp46, NKG2D, CD244, CD127, and intracellular Granzyme B in CD5$^+$NK1.1$^-$ γδ T cells, CD5$^-$NK1.1$^+$ γδ T cells from the liver of WT mice, and γδ T cells from liver of *flox/flox* mice. Bar graphs show mean fluorescence intensity (MFI) of each histogram.

(Figure S4C). These results suggest that CD5$^-$NK1.1$^+$ γδ T cells are not a fetal type and can develop in the adult thymus. Among γδ T cells developing in the adult thymus, γδ T cells developing directly from DN2a stage in a Bcl11b-independent manner are thought to be more primitive than those developing later from DN2b in a Bcl11b-dependent manner.

We further examined surface expression of CD5 and NK1.1 on γδ T cells from the liver of *CrehCD2*;*Rosa26*^{RFP} *Bcl11b*$^{flox/flox}$ mice. As marked by red fluorescent protein (RFP) expression due to excision of the loxP-flanked transcription-translation stop sequence from the *Rosa26*^{RFP} allele in *Rosa26*^{RFP} mice (Luche et al., 2007), hCD2-expressing mature T cells were RFP$^+$Bcl11b$^-$ in *CrehCD2*;*Rosa26*^{RFP} *Bcl11b*$^{flox/flox}$ mice. As shown in Figure S4D, RFP$^+$Bcl11b$^-$ γδ T cells were CD5$^+$NK1.1$^-$ (Figure S4D). These results suggest that unique CD5$^-$NK1.1$^+$ γδ T cells are primarily generated in the thymus and that CD5 down-regulation and NK1.1 acquisition may not occur in mature peripheral γδ T cells in the absence of Bcl11b.

Bcl11b-Independent γδ T Cells Participate in the Early Host Defense against Infection

We previously reported that γδ T cells have an important role in protection as early as 3 days after *L. monocytogenes* infection, which might bridge the gap between innate and adaptive immune activation following *L. monocytogenes* infection (Hiromatsu et al., 1992; Ohga et al., 1990). To determine whether γδ T cells are involved in early protection against *L. monocytogenes* infection, we examined γδ T cells in the liver of 3-week-old mice after intravenous inoculation with *L. monocytogenes*. At 3 days after infection, the major population of effector γδ T cells producing IFN-γ and/or Granzyme B was CD5$^-$NK1.1$^+$ γδ T cells. In contrast, at 5 days after infection, more effector cells had a CD5$^+$NK1.1$^-$ phenotype (Figures 6A–6C). Similar kinetics were also detected in the liver of 12-week-old mice following *L. monocytogenes* infection (Figures S5A–S5C). These results suggested that Bcl11b-independent CD5$^-$NK1.1$^+$ γδ T cells appeared before Bcl11b-dependent

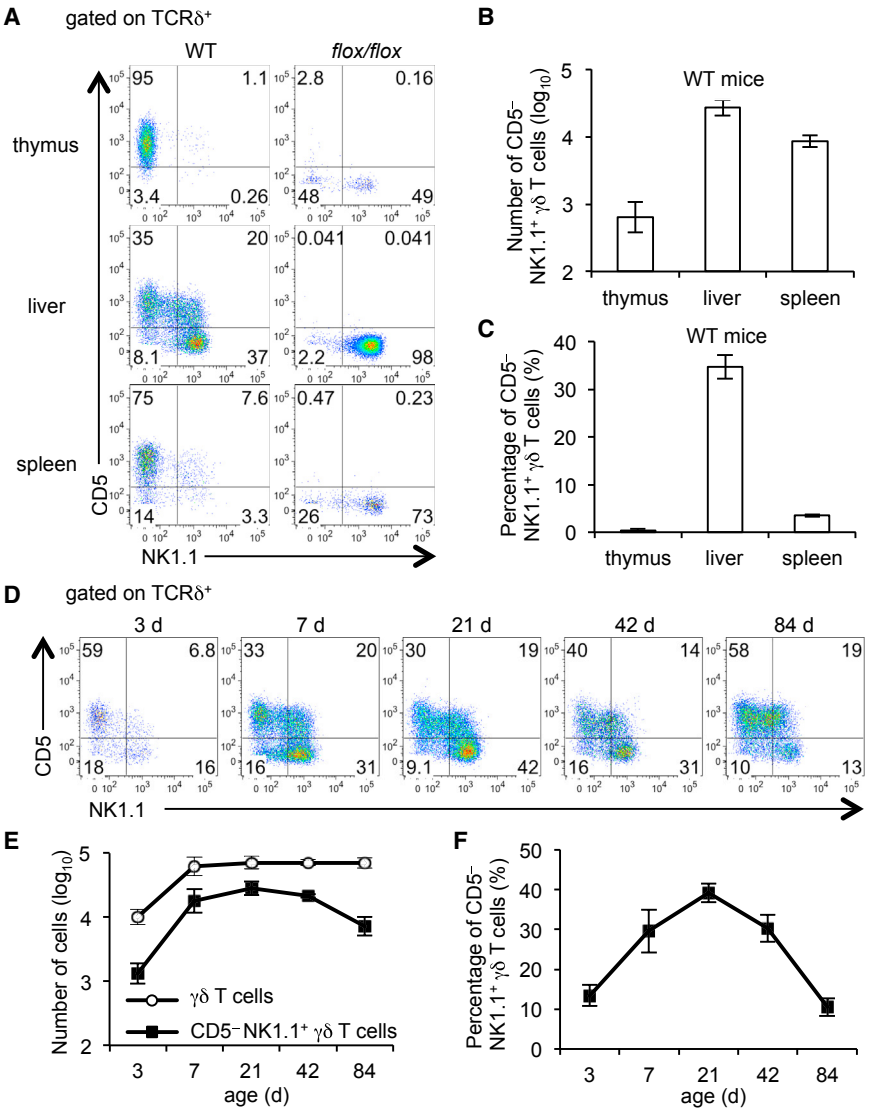

Figure 5. Tissue Distribution and Age-Related Changes in CD5⁻NK1.1⁺ γδ T Cells Numbers

(A) Representative dot plots are shown after gating on TCRδ⁺ cells. Numbers in the quadrants indicate the percentages of expression of CD5 and NK1.1 in γδ T cells of thymus, liver, and spleen from WT and *flox/flox* mice (n = 3).

(B) Bar graphs show the means ± SD of number of CD5⁻NK1.1⁺ γδ T cells in thymus, liver, and spleen from WT mice (n = 3).

(C) Bar graphs show the means ± SD of percentage of CD5⁻NK1.1⁺ γδ T cells in γδ T cells of thymus, liver, and spleen from WT mice (n = 3).

(D) Representative dot plots are shown after gating on TCRδ⁺ cells. Numbers in the quadrants indicate the percentages of expression of CD5 and NK1.1 in γδ T cells of liver from 3- to 84-day-old WT mice (n = 5).

(E) Line graphs show the means ± SD of number of γδ T cells and CD5⁻NK1.1⁺ γδ T cells from the liver of 3- to 84-day-old WT mice (n = 5).

(F) Line graphs show the means ± SD of percentages of CD5⁻NK1.1⁺ γδ T cells in γδ T cells from the liver of 3- to 84-day-old WT mice (n = 5).

See also Figures S3 and S4.

CD5⁺NK1.1⁻ γδ T cells after infection, resembling their sequential appearance during development in the thymus.

To investigate the potential role of Bcl11b-independent γδ T cells in early protection against *L. monocytogenes* infection, we examined bacterial growth in Cδ KO × *flox/flox* mice. Bacterial numbers in the liver and spleen were significantly higher in Cδ KO × *flox/flox* mice than in *flox/flox* mice on days 1 and 3 after infection (Figures 6D and S6). Thus, Bcl11b-independent γδ T cells contribute to protection in the early stages of *L. monocytogenes* infection. The bacterial numbers of WT mice were higher in the liver and spleen than *flox/flox* mice. This may be explained by the presence of relatively higher numbers of innate-like effector γδ T cells in *flox/flox* mice at the early stages after infection.

DISCUSSION

Here, we characterized the γδ T cell subset that develops from the DN2a stage in a Bcl11b-independent manner using *flox/flox* mice. RAG1/2 expression is known to begin at the transitional stage from DN1 and DN2a, during which Vγ–Jγ gene rearrangement occurs (Krangel, 2009). The *flox/flox* mice showed a complete absence of CD4⁺ CD8⁺ DP cells and very few αβ T cells but appreciable amounts of γδ T cells in the thymus. However, *flox/flox* mice generated only a limited amount of IFN-γ⁺ γδ T cells and no IL-17⁺ γδ T cells, which develop from DN2b cells in a Bcl11b-dependent manner, as previously observed in Bcl11b KO newborns (Rothenberg et al., 2008; Li et al., 2010a; Shibata et al., 2014). Deletion of Bcl11b in early CD4⁺ CD8⁺ DP thymocytes using CD4-Cre was reported to cause defects in Ca^{2+} influx (Albu et al., 2007). Consistent with this finding, we observed attenuated calcium influx in Bcl11b-deficient γδ T cells upon γδTCR stimulation. Taken together, *flox/flox* mice in which Bcl11b is completely blocked at the DN2a stage in thymic development are useful for analyzing primitive innate-like γδ T cells that develop before the DN2a stage in a Bcl11b-independent manner.

γδ T cells are present in small numbers in the blood and peripheral lymphoid tissues, but they are relatively abundant in s-IELs, r-IELs, and i-IELs (Asarnow et al., 1988; Goodman and Lefrancois, 1989; Havran and Allison, 1988; Hayday and Tigelaar, 2003). Both s-IELs and r-IELs differentiate in the thymus at a very early ontogenic stage, and they bear truly invariant Vγ5/Vδ1 or Vγ6/Vδ1 TCRs without junctional diversity (Itohara et al., 1990; Lafaille et al., 1989). Vγ5⁺ γδ T cells were equally

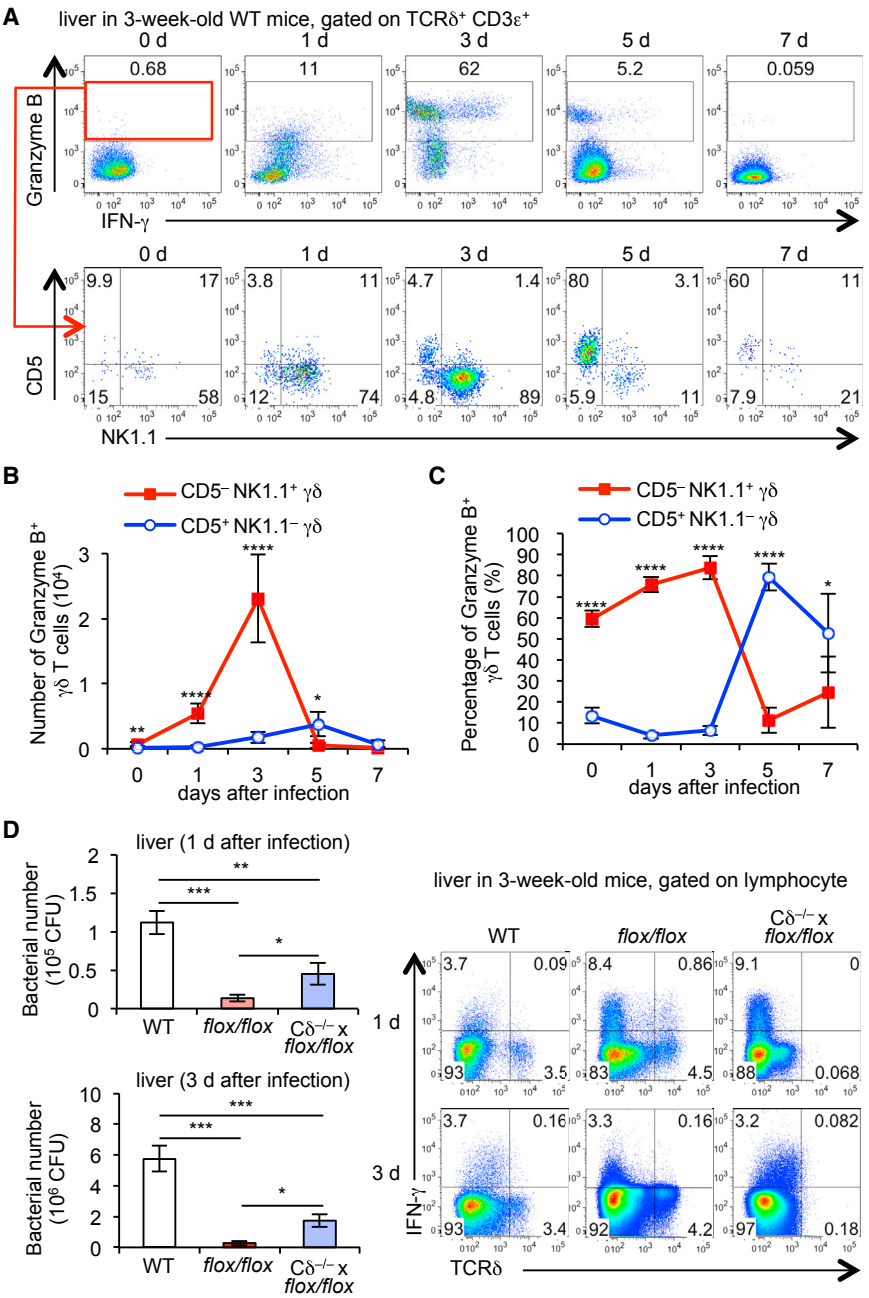

Figure 6. Bcl11b-Independent γδ T Cells of Liver Are Involved in Host Defense after *L. monocytogenes* Infection

(A) Kinetics of γδ T cells expressing Granzyme B and IFN-γ in the liver of 3-week-old WT mice after intravenous inoculation with *L. monocytogenes*. Upper dot plots are shown after gating on TCRδ$^+$CD3ε$^+$ cells. Numbers in the quadrants indicate the percentages of expression of intracellular Granzyme B and IFN-γ in γδ T cells of liver from WT mice. Lower dot plots are shown after gating on Granzyme B$^+$ γδ T cells. Numbers in the quadrants indicate the percentages of expression of CD5 and NK1.1. Data are representative of 5 mice from each group.

(B) Line graphs show the kinetics of number of CD5$^-$NK1.1$^+$ and CD5$^+$NK1.1$^-$ in Granzyme B$^+$ γδ T cells in the liver after infection. Each point and vertical bar is the mean ± SD of 5 mice.

(C) Line graphs show the kinetics of percentage of CD5$^-$NK1.1$^+$ and CD5$^+$NK1.1$^-$ in Granzyme B$^+$ γδ T cells from the liver after infection. Each point and vertical bar is the mean ± SD of 5 mice.

(D) Bar graphs show the means ± SD of bacterial number in the liver from WT, *flox/flox*, and Cδ$^{-/-}$ × *flox/flox* mice on days 1 (upper panel) and 3 (under panel) after *L. monocytogenes* infection (n = 3). Representative dot plots are shown after gating on lymphocyte. Numbers in the quadrants indicate the percentages of expression of intracellular IFN-γ and TCRδ in lymphocytes of liver from WT, *flox/flox*, and Cδ$^{-/-}$ × *flox/flox* mice on days 1 (upper panels) and 3 (under panels) after *L. monocytogenes* infection (n = 3).

Significant differences are shown (*$p < 0.05$, **$p < 0.01$, ***$p < 0.001$, and ****$p < 0.0001$; Student's t test, A–C, and one-way ANOVA/Tukey, D). See also Figures S5 and S6.

detected in s-IELs of *flox/flox* and *flox*/+ mice, confirming that this population can develop in the thymus at a very early ontogenic stage under Bcl11b-deficient conditions. Meanwhile, γδ T cells expressing Vγ6$^+$ mRNA or CD8αα γδ T cells were reduced in the r-IEL or i-IEL populations, respectively, of *flox/flox* mice. Despite early reports suggesting an extrathymic origin for i-IELs, recent studies indicate that the majority of CD8αα i-IELs are derived from thymic precursors, a unique CD8αα-expressing subset of CD4$^+$ CD8αβ$^+$ thymocytes, that subsequently migrate to the gut (Cheroutre et al., 2011). Our present results suggest that most CD8αα γδ i-IELs develop later than the DN2b stage in a Bcl11b-dependent manner, but a significant number of γδ T cells may originate from immature DN2a thymic precursors.

In the present study, γδ T cells from *flox/flox* mice notably expressed higher levels of NK1.1, NKp46, NKG2D, CD244, and Granzyme B, but no CD5 or CD127. The corresponding γδ T cells are present under physiological conditions in WT mice, especially in the liver of young mice. Using *CreERT2;Bcl11b$^{flox/flox}$* mice, in which tamoxifen-induced Cre recombinase is encoded in the ubiquitously expressed Rosa26 locus, Li et al. (2010b) found that Bcl11b-deficient DN1-2-3 thymocytes differentiate into cells of the NK-like lineage and express some NK-related genes, such as NK1.1, NKp46, and NKG2A/C/E, in vitro. Furthermore, even acute loss of Bcl11b by in vivo injection of tamoxifen increased the numbers of CD3$^-$NKp46$^+$ cells and CD3$^+$NKP46$^+$ T cells (including γδ T cells) in the thymus and spleen of adult mice (Li et al., 2010b). On the other hand, it was reported that using CD4-Cre, deletion of Bcl11b in early DP thymocytes induced

the expression of some genes usually expressed in mature single-positive T cells, such as *Zbtb7b* (*Th-POK*) and *Runx3*, but no NK cell genes (Kastner et al., 2010; Avram and Califano, 2014). We also showed that, using *CrehCD2*;*Rosa26*^{RFP} *Bcl11b*$^{flox/flox}$ mice, the acquisition of NK1.1 and downregulation of CD5 may not occur in mature T cells in peripheral tissues in the absence of Bcl11b. Hirose et al. (2015) recently reported that Bcl11b prevents the intrathymic development of innate-like CD8 T cells. Thus, Bcl11b has a role in repressing genes of the innate immune system, such as NK-related genes during T cell development in the thymus.

It is reported that deletion of *Bcl11b* in early DP thymocytes caused defects in the initiation of positive selection, including impaired proximal TCR signaling, attenuated extracellular signal-regulated kinase phosphorylation, and Ca^{2+} influx (Albu et al., 2007). Consistent with these findings, we observed attenuated Ca^{2+} influx in Bcl11b-deficient γδ T cells upon TCR stimulation. Bcl11b also may be involved in signaling pathways downstream of TCRs, such as Ca^{2+} influx. It remains unclear how Bcl11b represses NK-related genes and other precocious T cell profiles during T cell development. Recent advances in combinatorial action of Bcl11b with other transcription factors, such as E2A, Runx1, TCF-1, and GATA3, may clarify activation and repression target genes bound by Bcl11b (Longabaugh et al., 2017; Kueh et al., 2016).

CD5^{-}NK1.1^{+} γδ T cells that develop from early T cell precursor have an enormous potential to express IFN-γ and Granzyme B. Therefore, CD5^{-}NK1.1^{+} γδ T cells may provide early protection as part of innate immunity against microbial infection and tumor development, and they might thus bridge the gap between innate and adaptive immunity. Recently, Dadi et al. (2016) reported that innate-like unconventional T cells expressing NK1.1^{+} (including γδ T cells) engage in immunosurveillance during early tumor onset by responding to cell transformation. We found that Granzyme B^{+} CD5^{-}NK1.1^{+} γδ T cell numbers increased to reach a peak on day 3 following infection with *L. monocytogenes*, preceding the appearance of CD5^{+}NK1.1^{-} γδ T cells. We further found a potential role for Bcl11b-independent γδ T cells in early protection against *L. monocytogenes* in *flox/flox* mice genetically depleted of γδ T cells. These results suggest that Bcl11b-independent γδ T cells precede the appearance of Bcl11b-dependent γδ T cells during host defense against infection, resembling their sequential appearance during thymus development.

In conclusion, Bcl11b-independent γδ T cells had a CD5^{-}NK1.1^{+} Granzyme^{+} phenotype and were abundant in the liver in WT mice. Bcl11b-independent γδ T cells contributed to early protection against *L. monocytogenes* infection. Bcl11b-independent γδ T cells participated in early protection as primitive innate-like γδ T cells in host defense.

EXPERIMENTAL PROCEDURES

Mice

C57BL/6 female mice were purchased from Japan KBT (Tosu, Japan). *Bcl11b*$^{flox/flox}$ mice were provided by R. Kominami (Niigata University, Niigata, Japan) (Go et al., 2013). *CreRag1* mice were provided by T. Rabbitts (Leeds Institute of Molecular Medicine, Leeds, UK) courtesy of K. Akashi (Kyushu University, Fukuoka, Japan) (Forster et al., 2005). Cδ KO mice were generated as previously described (Itohara et al., 1993). *Bcl11b* conditional KO mice were generated by crossing *Bcl11b*$^{flox/flox}$ mice with *CreRag1* mice (*CreRag1*;*Bcl11b*$^{flox/flox}$ mice). *CrehCD2* mice were purchased from Jackson Laboratory (Bar Harbor, ME, USA). *CrehCD2* mice were crossed to mice expressing an allele for the expression of RFP from the ubiquitously expressed Rosa26 locus (Rosa26-STOP-RFP; called *Rosa26*^{RFP}) (Luche et al., 2007). *CrehCD2*;*Rosa26*^{RFP} *Bcl11b*$^{flox/flox}$ mice were generated by crossing *CrehCD2*;*Rosa26*^{RFP} mice with *Bcl11b*$^{flox/flox}$ mice. For γδ T cell-deficient *Bcl11b* conditional KO mice, *CreRag1*;*Bcl11b*$^{flox/flox}$ mice were backcrossed with Cδ KO mice. All mice were female and used at 3, 7, 21, 42, or 84 days of age. All mice were maintained under specific pathogen-free conditions and provided with food and water ad libitum. Age- and gender-matched mice were used for all experiments. This study was approved by the Committee of Ethics on Animal Experiments of the Faculty of Medicine, Kyushu University. Experiments were carried out according to local guidelines for animal experimentation.

Cell Preparations from Various Tissues

Single-cell suspensions were isolated from the thymus, uterus, PEC, i-IEL, colonic lamina propria lymphocytes (c-LPL), lung, and spleen as previously described (Shibata et al., 2008). Livers were homogenized using slide glasses and passed through a mesh, and mononuclear cells were further purified with 40% and 70% Percoll (GE Healthcare Bio-Sciences AB, Uppsala, Sweden) by centrifugation at 600 × *g* for 20 min. Epidermal sheets were isolated from the ear as previously described (Haas et al., 2012). s-IELs were isolated from epidermal sheets of ears by centrifugation in a 40% and 70% Percoll gradient.

Flow Cytometry Analysis

Cells were stained for 20 min at 4°C with mAbs. We added 1 μg/mL propidium iodide (Sigma-Aldrich, Tokyo, Japan) to the cell suspension just before flow cytometry to detect and exclude dead cells from the analysis of surface staining. To measure cytokine production, cells were stimulated with 25 ng/mL PMA (Sigma-Aldrich) and 1 μg/mL ionomycin (Sigma-Aldrich) for 4 hr at 37°C; 10 μg/mL Brefeldin A (Sigma-Aldrich) was added for the last 3 hr of incubation. After cells were stained with various mAbs, intracellular staining was performed according to the manufacturer's instructions (BD Biosciences, San Jose, CA, USA). 100 μL BD Cytofix/Cytoperm solution (BD Biosciences) was added to the cell suspension with gentle mixing and incubated for 20 min at 4°C. Fixed cells were washed twice with 250 μL 10% BD Perm/Wash solution (BD Biosciences) and then stained intracellularly for 30 min at 4°C. Stained cells were analyzed on a FACSVerse flow cytometer (BD Biosciences), and data were analyzed using FlowJo software (Tree Star, Ashland, OR, USA). We used the nomenclature of Heilig and Tonegawa (1986) for TCR γ chains.

Antibodies for flow cytometry analysis are detailed in the Supplemental Experimental Procedures.

γδ T Cell Sorting

Single-cell suspensions were isolated from various tissues and stained with mAbs. γδ T cells, CD5^{+}NK1.1^{-} γδ T cells, and CD5^{-}NK1.1^{+}γδ T cells were sorted using a FACSAria (BD Biosciences).

Measurement of Ca^{2+} Mobilization

Single-cell suspensions were prepared from a mouse thymus. CD4^{+}, CD8^{+}, and major histocompatibility complex (MHC) class II^{+} thymocytes were depleted by negative selection with anti-CD4 (GK1.5, BioLegend, San Diego, CA. USA), anti-CD8α (53-6.7, BioLegend), and anti-MHC class II (M5/114.15.2, BioLegend) mAbs, followed by incubation with anti-Rat IgG Dynabeads (Invitrogen, Carlsbad, CA, USA). Purified cells were loaded with 10 μM membrane-permeable fluorescent Ca^{2+} indicator dye Cal-520 AM (AAT Bioquest, Sunnyvale, CA, USA) and 10 μM Fura-red AM (Thermo Fisher Scientific, Waltham, MA, USA) for 30 min at 37°C. Cells were then stained with anti-TCRδ (GL3) mAb and incubated on ice. Before stimulation, cell aliquots were equilibrated to 37°C for 5 min and then analyzed using a FACSCalibur flow cytometer (BD Biosciences) and FACSVerse flow cytometer. After acquisition of background intracellular Ca^{2+} concentrations for 30 s, cells were stimulated via the TCR with biotinylated anti-CD3ε (145-2C11), streptavidin (20 μg/mL)

was crosslinked to the TCR, and cell responses were assayed for 5 min. Data were analyzed using FlowJo software.

ELISA

After single-cell suspensions were prepared from the thymus of *flox*/+ and *flox/flox* mice, thymocytes (2×10^4 cells/well) were stimulated with anti-TCRδ mAb (GL3) in the presence of anti-Hamster IgG (10 μg/well) for crosslinking. After stimulation, IL-17A and IFN-γ levels in 3-day culture supernatants were analyzed with a DuoSet ELISA Development System (R&D Systems), according to the manufacturer's instructions.

Immunohistochemistry

Ear epidermal layers were prepared on glass slides, fixed with phosphate-buffered 4% paraformaldehyde (Nacalai Tesque, Kyoto, Japan) at room temperature (RT) for 10 min, permeabilized with rinse buffer (50 mM Tris-HCL and 0.1% Triton-X [pH 8.0]) for 10 min, and blocked with Blocking One Histo (Nacalai Tesque) at RT for 10 min. Epidermal sheets were then incubated with the following antibodies diluted in blocking solution (1 × Tris-buffered saline, 0.1% Tween 20 [Sigma-Aldrich], and 5% Blocking One Histo) at 4°C overnight: 1:100 dilution Alexa Fluor 647-conjugated anti-CD3ε mAb (17A2) and 1:100 dilution phycoerythrin (PE)-conjugated anti-Vγ5 mAb (536). Slides were mounted in ProLong Gold Antifade reagent (Invitrogen) and analyzed with a Zeiss LSM700 confocal microscope (Carl Zeiss, Oberkochen, Germany).

RNA Purification and RT-PCR

Total RNA was purified from sorted γδ T cells using an RNeasy Mini Kit (QIAGEN, Hilden, Germany), and cDNA was synthesized using Superscript II (Invitrogen) according to the manufacturer's instructions. PCR was performed on a PCR thermal cycler (Takara, Tokyo, Japan). RT-PCR products were analyzed by blotting in 1.8% agarose gels.

Primers for RT-PCR are detailed in the Supplemental Experimental Procedures.

Gene Expression Microarrays

Total RNA was isolated from sorted $CD5^-NK1.1^+$ and $CD5^+NK1.1^-$ γδ T cells from the livers of WT mice or γδ T cells from the livers of *flox/flox* mice using an RNeasy Mini Kit (QIAGEN), according to the manufacturer's instructions. RNA samples were quantified using an ND-1000 spectrophotometer (NanoDrop Technologies, Wilmington, DE), and RNA quality was confirmed with a 2200 TapeStation (Agilent Technologies, Santa Clara, CA). cRNA was amplified, labeled with 10 ng total RNA using a GeneChip WT Pico Kit, and hybridized to an Affymetrix GeneChip Mouse Gene 2.0 ST Array, according to the manufacturer's instructions. Hybridized microarrays were then scanned with an Affymetrix scanner. Relative hybridization intensities and background hybridization values were calculated using Affymetrix Expression Console. The raw signal intensities for all samples were normalized by quantile algorithm with Affymetrix Power Tool version 1.15.0 software. To identify up- or downregulated genes, we calculated the *Z* scores (Quackenbush, 2002) and ratios (non-log-scale fold change) from the normalized signal intensities for each probe to compare control and experimental samples. Criteria used for identifying up- and downregulated genes were as follows: upregulated genes, Z score $\geq$ 2.0 and ratio $\geq$ 2.0; downregulated genes, Z score ≤ -2.0 and ratio $\leq$ 0.5. A heatmap was generated with MeV software (Saeed et al., 2003). The color indicates the distance from the mean of each probe intensity ($\log_2$ transformed). Microarray data analysis was supported by Cell Innovator (Fukuoka, Japan).

Generation of BM and Fetal Liver Chimera

BM cells were extracted from 8-week-old WT mice (Ly5.2/5.2) by flushing femurs and tibias, and they were then depleted of T cells using anti-CD3 mAb (17A2, BioLegend) and anti-Rat IgG Dynabeads. FL cells were extracted from liver of E14 WT mice (Ly5.2/5.2). 2×10^7 BM cells or 5×10^6 FL cells were intravenously injected into lethally irradiated (10 Gy) recipient 8-week-old WT mice (Ly5.1/5.1). After 8 weeks, reconstitution was confirmed.

Microorganisms and Bacterial Infection

The *L. monocytogenes* EGD strain was inoculated into C57BL/6 mice, and fresh single colonies were obtained from infected spleen after plating onto Trypto-Soya Agar (Nissui, Tokyo, Japan). Single colonies were picked and grown with vigorous shaking in 250 mL Trypto-Soya Broth (Nissui) at 37°C for 15 hr. Bacteria were stored in 50% glycerol (Sigma-Aldrich, Tokyo, Japan) at −80°C until use. Mice were intravenously infected with 4×10^5 colony-forming units (CFUs) of *L. monocytogenes*, corresponding to 1/10 of the 50% lethal dose (LD50) for C57BL/6 mice. At the indicated times after infection, bacterial numbers were counted as CFUs after incubation at 37°C.

Statistical Analysis

Statistical significance was evaluated using Prism software (GraphPad, San Diego, CA). Student's t test was used when only two groups were compared, and one-way ANOVA/Tukey was used for multiple comparisons. p values < 0.05 were considered to represent significant differences.

DATA AND SOFTWARE AVAILABILITY

The accession number for the microarray data reported in this paper is GEO: GSE89906. The accession number for the flow cytometry data reported in this paper is Flow Repository: FR-FCM-ZYBN.

SUPPLEMENTAL INFORMATION

Supplemental Information includes Supplemental Experimental Procedures and six figures and can be found with this article online at https://doi.org/10.1016/j.celrep.2017.10.007.

AUTHOR CONTRIBUTIONS

Y.Y. and S.H. designed the experiments and wrote the manuscript. S.H. conducted the experiments and analyzed data. T.M., N.N., and H.Y. provided feedback and expertise. All authors participated in discussions of the experiments, the results, and the manuscript.

ACKNOWLEDGMENTS

The authors are grateful to R. Kominami, T. Rabbits, H.J. Fehling, H. Luche, and K. Shibata for providing reagents and protocols and Y. Kitada, A. Yano, and N. Kurisaki for helping to prepare the manuscript. This work was supported by a Grant-in-Aid for Scientific Research on Innovative Areas JSPS KAKENHI (JP 16H06496) and a Grant-in-Aid for Scientific Research B JSPS KAKENHI (JP 26293098).

Received: March 24, 2017
Revised: September 1, 2017
Accepted: October 2, 2017
Published: October 31, 2017

REFERENCES

Albu, D.I., Feng, D., Bhattacharya, D., Jenkins, N.A., Copeland, N.G., Liu, P., and Avram, D. (2007). BCL11B is required for positive selection and survival of double-positive thymocytes. J. Exp. Med. *204*, 3003–3015.

Asarnow, D.M., Kuziel, W.A., Bonyhadi, M., Tigelaar, R.E., Tucker, P.W., and Allison, J.P. (1988). Limited diversity of gamma delta antigen receptor genes of Thy-1^+ dendritic epidermal cells. Cell *55*, 837–847.

Avram, D., and Califano, D. (2014). The multifaceted roles of Bcl11b in thymic and peripheral T cells: impact on immune diseases. J. Immunol. *193*, 2059–2065.

Avram, D., Fields, A., Senawong, T., Topark-Ngarm, A., and Leid, M. (2002). COUP-TF (chicken ovalbumin upstream promoter transcription factor)-interacting protein 1 (CTIP1) is a sequence-specific DNA binding protein. Biochem. J. *368*, 555–563.

Bonneville, M., Janeway, C.A., Jr., Ito, K., Haser, W., Ishida, I., Nakanishi, N., and Tonegawa, S. (1988). Intestinal intraepithelial lymphocytes are a distinct set of gamma delta T cells. Nature *336*, 479–481.

Cheroutre, H., Lambolez, F., and Mucida, D. (2011). The light and dark sides of intestinal intraepithelial lymphocytes. Nat. Rev. Immunol. *11*, 445–456.

Chien, Y.H., Meyer, C., and Bonneville, M. (2014). γδ T cells: first line of defense and beyond. Annu. Rev. Immunol. *32*, 121–155.

Dadi, S., Chhangawala, S., Whitlock, B.M., Franklin, R.A., Luo, C.T., Oh, S.A., Toure, A., Pritykin, Y., Huse, M., Leslie, C.S., and Li, M.O. (2016). Cancer Immunosurveillance by Tissue-Resident Innate Lymphoid Cells and Innate-like T Cells. Cell *164*, 365–377.

Forster, A., Pannell, R., Drynan, L.F., Codrington, R., Daser, A., Metzler, M., Lobato, M.N., and Rabbitts, T.H. (2005). The invertor knock-in conditional chromosomal translocation mimic. Nat. Methods *2*, 27–30.

Go, R., Hirose, S., Katsuragi, Y., Obata, M., Abe, M., Mishima, Y., Sakimura, K., and Kominami, R. (2013). Cell of origin in radiation-induced premalignant thymocytes with differentiation capability in mice conditionally losing one Bcl11b allele. Cancer Sci. *104*, 1009–1016.

Goodman, T., and Lefrancois, L. (1989). Intraepithelial lymphocytes. Anatomical site, not T cell receptor form, dictates phenotype and function. J. Exp. Med. *170*, 1569–1581.

Haas, J.D., Ravens, S., Düber, S., Sandrock, I., Oberdörfer, L., Kashani, E., Chennupati, V., Föhse, L., Naumann, R., Weiss, S., et al. (2012). Development of interleukin-17-producing γδ T cells is restricted to a functional embryonic wave. Immunity *37*, 48–59.

Havran, W.L., and Allison, J.P. (1988). Developmentally ordered appearance of thymocytes expressing different T-cell antigen receptors. Nature *335*, 443–445.

Hayday, A.C., and Pennington, D.J. (2007). Key factors in the organized chaos of early T cell development. Nat. Immunol. *8*, 137–144.

Hayday, A., and Tigelaar, R. (2003). Immunoregulation in the tissues by gammadelta T cells. Nat. Rev. Immunol. *3*, 233–242.

Heilig, J.S., and Tonegawa, S. (1986). Diversity of murine gamma genes and expression in fetal and adult T lymphocytes. Nature *322*, 836–840.

Hiromatsu, K., Yoshikai, Y., Matsuzaki, G., Ohga, S., Muramori, K., Matsumoto, K., Bluestone, J.A., and Nomoto, K. (1992). A protective role of gamma/delta T cells in primary infection with *Listeria monocytogenes* in mice. J. Exp. Med. *175*, 49–56.

Hirose, S., Touma, M., Go, R., Katsuragi, Y., Sakuraba, Y., Gondo, Y., Abe, M., Sakimura, K., Mishima, Y., and Kominami, R. (2015). Bcl11b prevents the intrathymic development of innate CD8 T cells in a cell intrinsic manner. Int. Immunol. *27*, 205–215.

Ikawa, T., Hirose, S., Masuda, K., Kakugawa, K., Satoh, R., Shibano-Satoh, A., Kominami, R., Katsura, Y., and Kawamoto, H. (2010). An essential developmental checkpoint for production of the T cell lineage. Science *329*, 93–96.

Inoue, J., Kanefuji, T., Okazuka, K., Watanabe, H., Mishima, Y., and Kominami, R. (2006). Expression of TCR alpha beta partly rescues developmental arrest and apoptosis of alpha beta T cells in Bcl11b$^{-/-}$ mice. J. Immunol. *176*, 5871–5879.

Itohara, S., Farr, A.G., Lafaille, J.J., Bonneville, M., Takagaki, Y., Haas, W., and Tonegawa, S. (1990). Homing of a gamma delta thymocyte subset with homogeneous T-cell receptors to mucosal epithelia. Nature *343*, 754–757.

Itohara, S., Mombaerts, P., Lafaille, J., Iacomini, J., Nelson, A., Clarke, A.R., Hooper, M.L., Farr, A., and Tonegawa, S. (1993). T cell receptor delta gene mutant mice: independent generation of alpha beta T cells and programmed rearrangements of gamma delta TCR genes. Cell *72*, 337–348.

Kastner, P., Chan, S., Vogel, W.K., Zhang, L.J., Topark-Ngarm, A., Golonzhka, O., Jost, B., Le Gras, S., Gross, M.K., and Leid, M. (2010). Bcl11b represses a mature T-cell gene expression program in immature CD4(+)CD8(+) thymocytes. Eur. J. Immunol. *40*, 2143–2154.

Krangel, M.S. (2009). Mechanics of T cell receptor gene rearrangement. Curr. Opin. Immunol. *21*, 133–139.

Kueh, H.Y., Yui, M.A., Ng, K.K., Pease, S.S., Zhang, J.A., Damle, S.S., Freedman, G., Siu, S., Bernstein, I.D., Elowitz, M.B., and Rothenberg, E.V. (2016). Asynchronous combinatorial action of four regulatory factors activates Bcl11b for T cell commitment. Nat. Immunol. *17*, 956–965.

Lafaille, J.J., DeCloux, A., Bonneville, M., Takagaki, Y., and Tonegawa, S. (1989). Junctional sequences of T cell receptor gamma delta genes: implications for gamma delta T cell lineages and for a novel intermediate of V-(D)-J joining. Cell *59*, 859–870.

Li, L., Leid, M., and Rothenberg, E.V. (2010a). An early T cell lineage commitment checkpoint dependent on the transcription factor Bcl11b. Science *329*, 89–93.

Li, P., Burke, S., Wang, J., Chen, X., Ortiz, M., Lee, S.C., Lu, D., Campos, L., Goulding, D., Ng, B.L., et al. (2010b). Reprogramming of T cells to natural killer-like cells upon Bcl11b deletion. Science *329*, 85–89.

Liu, P., Li, P., and Burke, S. (2010). Critical roles of Bcl11b in T-cell development and maintenance of T-cell identity. Immunol. Rev. *238*, 138–149.

Longabaugh, W.J.R., Zeng, W., Zhang, J.A., Hosokawa, H., Jansen, C.S., Li, L., Romero-Wolf, M., Liu, P., Kueh, H.Y., Mortazavi, A., and Rothenberg, E.V. (2017). Bcl11b and combinatorial resolution of cell fate in the T-cell gene regulatory network. Proc. Natl. Acad. Sci. USA *114*, 5800–5807.

Luche, H., Weber, O., Nageswara Rao, T., Blum, C., and Fehling, H.J. (2007). Faithful activation of an extra-bright red fluorescent protein in "knock-in" Cre-reporter mice ideally suited for lineage tracing studies. Eur. J. Immunol. *37*, 43–53.

Mokuno, Y., Matsuguchi, T., Takano, M., Nishimura, H., Washizu, J., Ogawa, T., Takeuchi, O., Akira, S., Nimura, Y., and Yoshikai, Y. (2000). Expression of toll-like receptor 2 on gamma delta T cells bearing invariant V gamma 6/V delta 1 induced by *Escherichia coli* infection in mice. J. Immunol. *165*, 931–940.

Mombaerts, P., Arnoldi, J., Russ, F., Tonegawa, S., and Kaufmann, S.H.E. (1993). Different roles of alpha beta and gamma delta T cells in immunity against an intracellular bacterial pathogen. Nature *365*, 53–56.

Ohga, S., Yoshikai, Y., Takeda, Y., Hiromatsu, K., and Nomoto, K. (1990). Sequential appearance of gamma/delta- and alpha/beta-bearing T cells in the peritoneal cavity during an i.p. infection with *Listeria monocytogenes*. Eur. J. Immunol. *20*, 533–538.

Petrie, H.T., Scollay, R., and Shortman, K. (1992). Commitment to the T cell receptor-alpha beta or -gamma delta lineages can occur just prior to the onset of CD4 and CD8 expression among immature thymocytes. Eur. J. Immunol. *22*, 2185–2188.

Prinz, I., Sansoni, A., Kissenpfennig, A., Ardouin, L., Malissen, M., and Malissen, B. (2006). Visualization of the earliest steps of gammadelta T cell development in the adult thymus. Nat. Immunol. *7*, 995–1003.

Quackenbush, J. (2002). Microarray data normalization and transformation. Nat. Genet. *32* (*Suppl*), 496–501.

Ribot, J.C., deBarros, A., Pang, D.J., Neves, J.F., Peperzak, V., Roberts, S.J., Girardi, M., Borst, J., Hayday, A.C., Pennington, D.J., and Silva-Santos, B. (2009). CD27 is a thymic determinant of the balance between interferon-gamma- and interleukin 17-producing gammadelta T cell subsets. Nat. Immunol. *10*, 427–436.

Rothenberg, E.V., Moore, J.E., and Yui, M.A. (2008). Launching the T-cell-lineage developmental programme. Nat. Rev. Immunol. *8*, 9–21.

Saeed, A.I., Sharov, V., White, J., Li, J., Liang, W., Bhagabati, N., Braisted, J., Klapa, M., Currier, T., Thiagarajan, M., et al. (2003). TM4: a free, open-source system for microarray data management and analysis. Biotechniques *34*, 374–378.

Satterwhite, E., Sonoki, T., Willis, T.G., Harder, L., Nowak, R., Arriola, E.L., Liu, H., Price, H.P., Gesk, S., Steinemann, D., et al. (2001). The BCL11 gene family: involvement of BCL11A in lymphoid malignancies. Blood *98*, 3413–3420.

Shibata, K., Yamada, H., Nakamura, R., Sun, X., Itsumi, M., and Yoshikai, Y. (2008). Identification of CD25^{+} gamma delta T cells as fetal thymus-derived naturally occurring IL-17 producers. J. Immunol. *181*, 5940–5947.

Shibata, K., Yamada, H., Nakamura, M., Hatano, S., Katsuragi, Y., Kominami, R., and Yoshikai, Y. (2014). IFN-γ-producing and IL-17-producing γδ T cells differentiate at distinct developmental stages in murine fetal thymus. J. Immunol. *192*, 2210–2218.

Skeen, M.J., and Ziegler, H.K. (1993). Induction of murine peritoneal gamma/delta T cells and their role in resistance to bacterial infection. J. Exp. Med. *178*, 971–984.

Vantourout, P., and Hayday, A. (2013). Six-of-the-best: unique contributions of γδ T cells to immunology. Nat. Rev. Immunol. *13*, 88–100.

Wakabayashi, Y., Inoue, J., Takahashi, Y., Matsuki, A., Kosugi-Okano, H., Shinbo, T., Mishima, Y., Niwa, O., and Kominami, R. (2003a). Homozygous deletions and point mutations of the Rit1/Bcl11b gene in gamma-ray induced mouse thymic lymphomas. Biochem. Biophys. Res. Commun. *301*, 598–603.

Wakabayashi, Y., Watanabe, H., Inoue, J., Takeda, N., Sakata, J., Mishima, Y., Hitomi, J., Yamamoto, T., Utsuyama, M., Niwa, O., et al. (2003b). Bcl11b is required for differentiation and survival of alphabeta T lymphocytes. Nat. Immunol. *4*, 533–539.

Yui, M.A., and Rothenberg, E.V. (2014). Developmental gene networks: a triathlon on the course to T cell identity. Nat. Rev. Immunol. *14*, 529–545.

Cell Reports, Volume *21*

Supplemental Information

$CD5^{-}NK1.1^{+}$ γδ T Cells that Develop in a Bcl11b-Independent Manner Participate in Early Protection against Infection

Shinya Hatano, Tesshin Murakami, Naoto Noguchi, Hisakata Yamada, and Yasunobu Yoshikai

SUPPLEMENTAL FIGURES

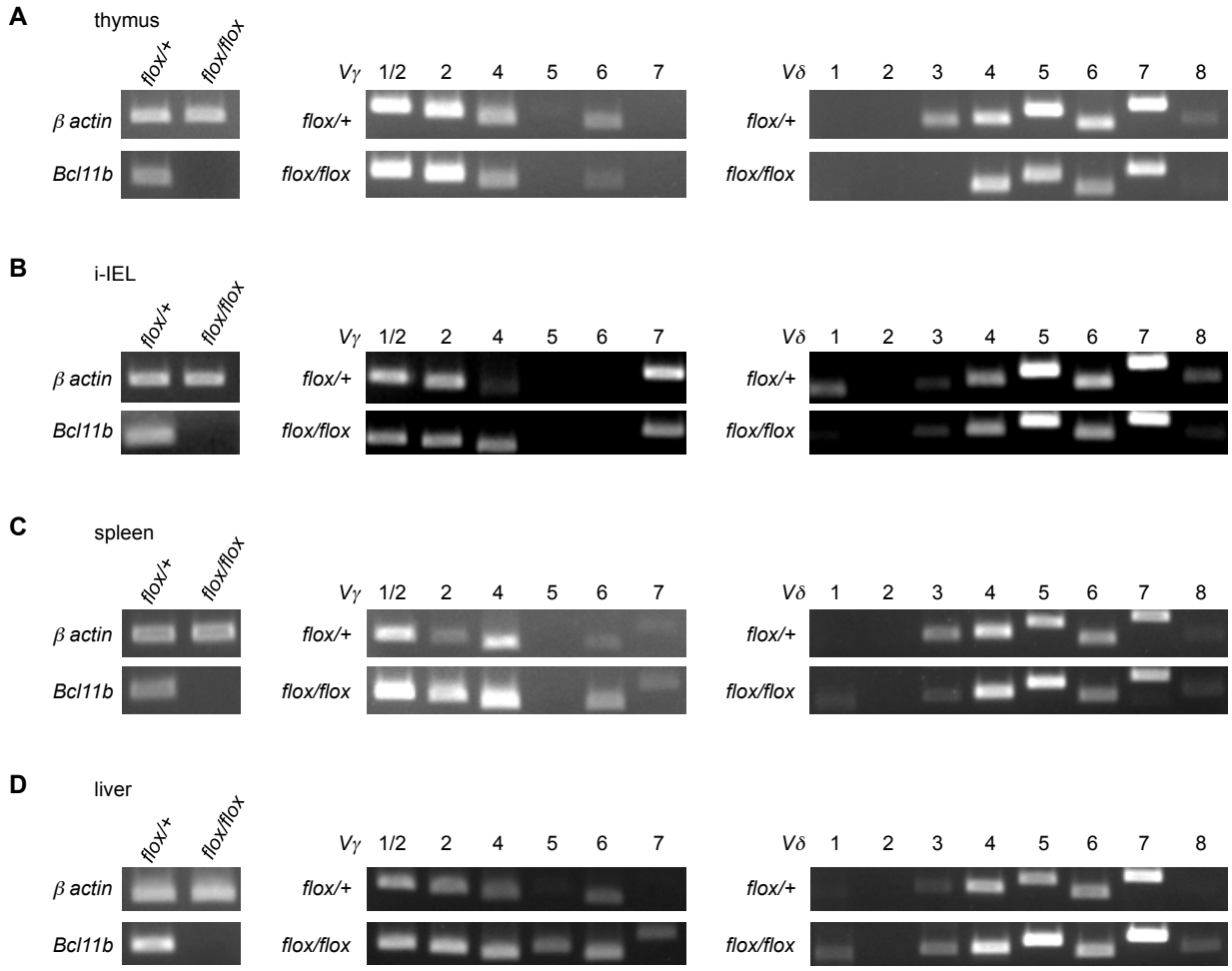

Supplemental Figure 1. Gene expression of TCR V repertoire in γδ T cells from *flox/+* and *flox/flox* mice (related to Figures 1 and 2)

(A–D) Gene expression of *Bcl11b*, TCR Vγ and Vδ repertoires in γδ T cells were analyzed in thymus (A), i-IEL (B), spleen (C), and liver (D) from *flox/+* and *flox/flox* mice.

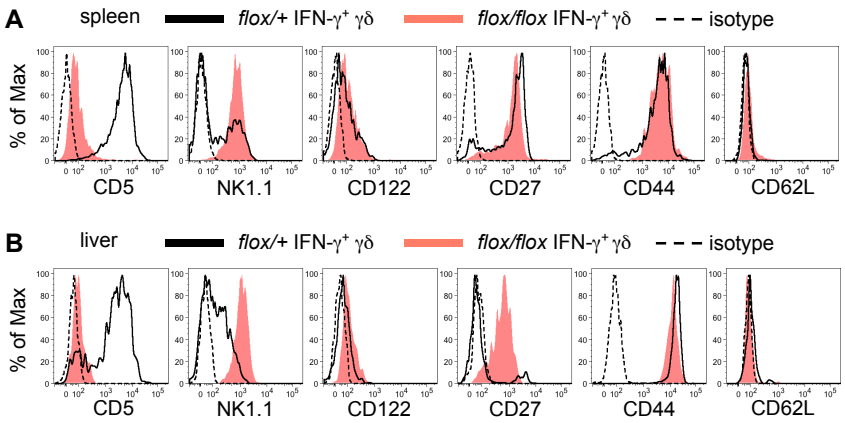

Supplemental Figure 2. Surface characteristics of IFN-γ$^+$ Bcl11b-independent γδ T cells (related to Figure 3)

(A and B) Histograms show expression of CD5, NK1.1, CD122, CD27, CD44, and CD62L on IFN-γ$^+$ γδ T cells of the spleen (A) and liver (B) from *flox/+* and *flox/flox* mice after PMA/ionomycin stimulation.

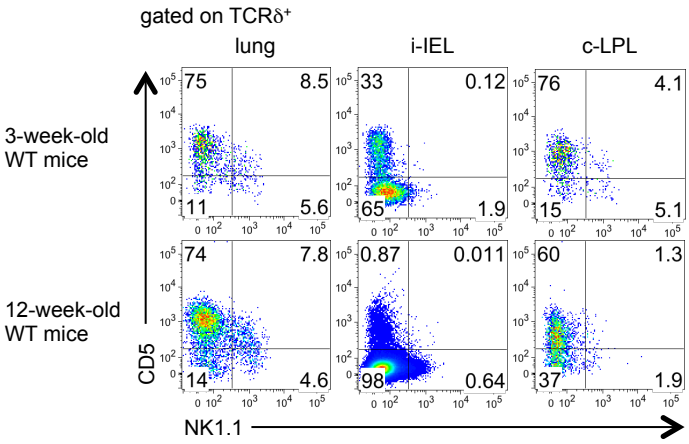

Supplemental Figure 3. The distribution of CD5$^-$ NK1.1$^+$ γδ T cells in lung and gut (related to Figure 5)

Representative dot plots are shown after gating on TCRδ$^+$ cells. Numbers in the quadrants indicate the percentage of expression of CD5 and NK1.1 in γδ T cells of lung, i-IEL and colonic lamina propria lymphocytes (c-LPL) from 3-week-old and 12-week-old WT mice (n = 4).

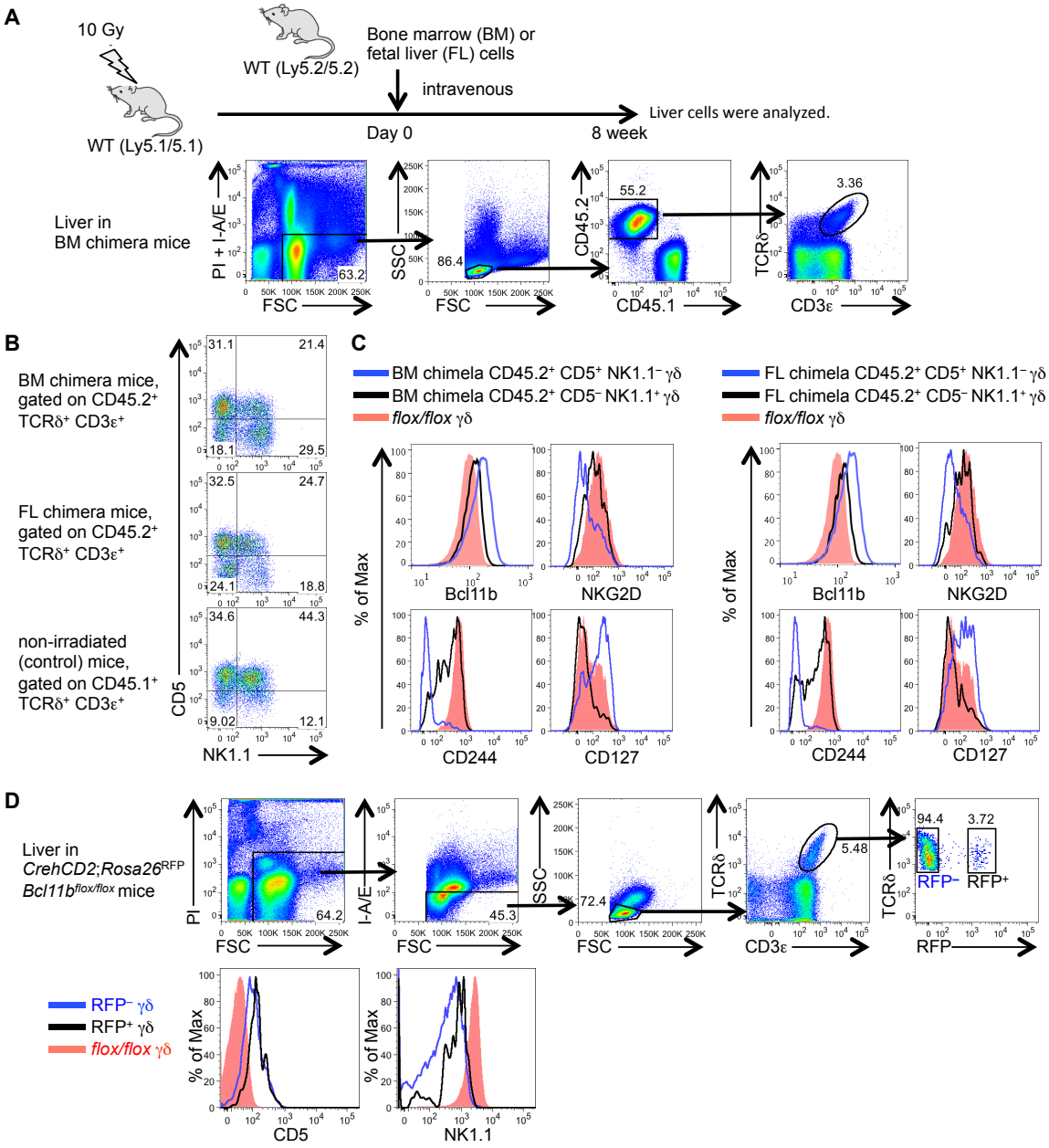

Supplemental Figure 4. Bcl11b-indenepndent CD5$^-$NK1.1$^+$ γδ T cells develop in adult thymus (related to Figure 5)

(A) Recipient WT (Ly5.1/5.1) mice were lethally irradiated and reconstituted by BM or FL cells from WT (Ly5.2/5.2) mice. Dot plots show an example of a gating strategy to identify γδ T cells derived from BM in the liver from BM chimera mice.

(B) Representative dot plots are shown after gating on CD45.2$^+$ TCRδ$^+$ CD3ε$^+$ cells. Numbers in the quadrants indicate the percentage of expression of CD5 and NK1.1 in γδ T cells of liver from BM and FL chimera mice (n =3).

(C) Histograms show expression of intracellular Bcl11b, NKG2D, CD244 and CD127 in CD45.2$^+$ CD5$^+$ NK1.1$^-$ γδ T cells, CD45.2$^+$ CD5$^-$ NK1.1$^+$ γδ T cells from the liver in BM and FL chimera mice and γδ T cells from the liver from *flox/flox* mice.

(D) Dot plots show an example of a gating strategy to identify RFP$^-$ γδ T and RFP$^+$ γδ T cells in the liver from *CrehCD2;Rosa26*^{RFP} *Bcl11b*$^{flox/flox}$ mice. Histograms show expression of CD5 and NK1.1 in RFP$^-$ γδ T cells, RFP$^+$ γδ T cells from *CrehCD2;Rosa26*^{RFP} *Bcl11b*$^{flox/flox}$ mice and γδ T cells from *flox/flox* mice.

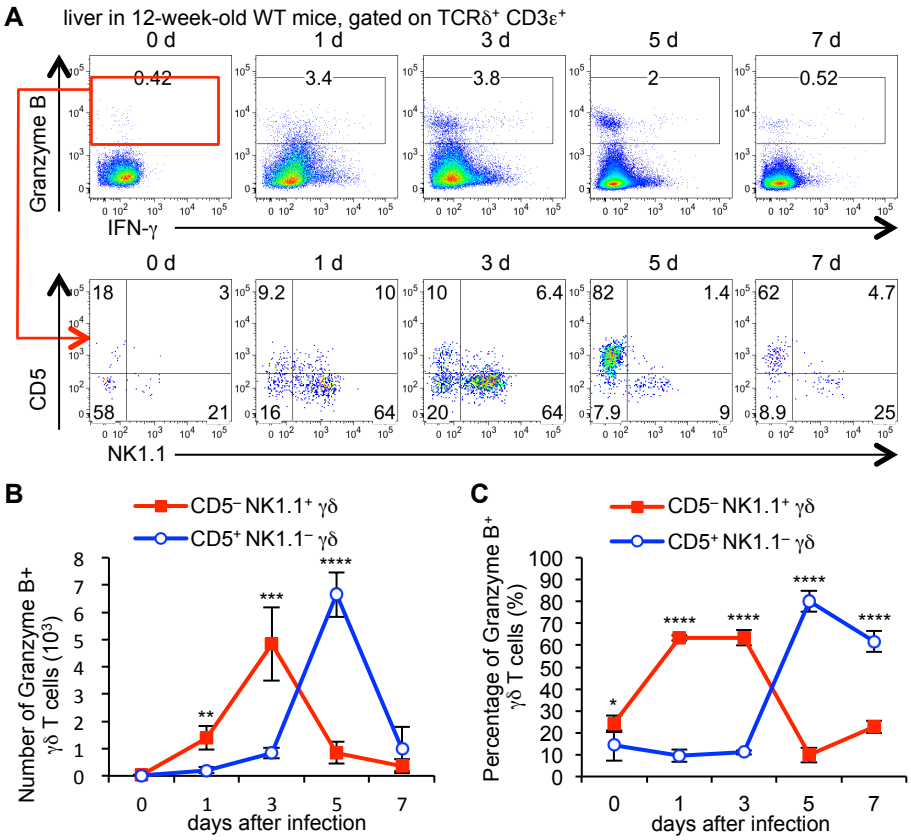

Supplemental Figure 5. Bcl11b-independent γδ T cells of the liver from 12-week-old WT mice are involved in host defense after *L. monocytogenes* infection (related to Figure 6)

(A) Kinetics of γδ T cells expressing IFN-γ and Granzyme B in the liver of 12-week-old WT mice after intravenous inoculation with *L. monocytogenes*. Upper dot plots are shown after gating on TCRδ$^+$ CD3ε$^+$ cells. Numbers in the quadrants indicate the percentage of expression of intracellular Granzyme B and IFN-γ in γδ T cells of liver. Lower dot plots are shown after gating on Granzyme B$^+$ γδ T cells. Numbers in the quadrants indicate the percentage of CD5 and NK1.1 expression. Data are representative of 4 mice from each group.

(B) Line graphs show the kinetics of number of CD5$^-$ NK1.1$^+$ and CD5$^+$ NK1.1$^-$ in Granzyme B$^+$ γδ T cells in the liver after infection. Each point and vertical bar is the mean ± SD of 4 mice.

(C) Line graphs show the kinetics of percentage of CD5$^-$ NK1.1$^+$ and CD5$^+$ NK1.1$^-$ in Granzyme B$^+$ γδ T cells from the liver after infection. Each point and vertical bar is the mean ± SD of 4 mice.

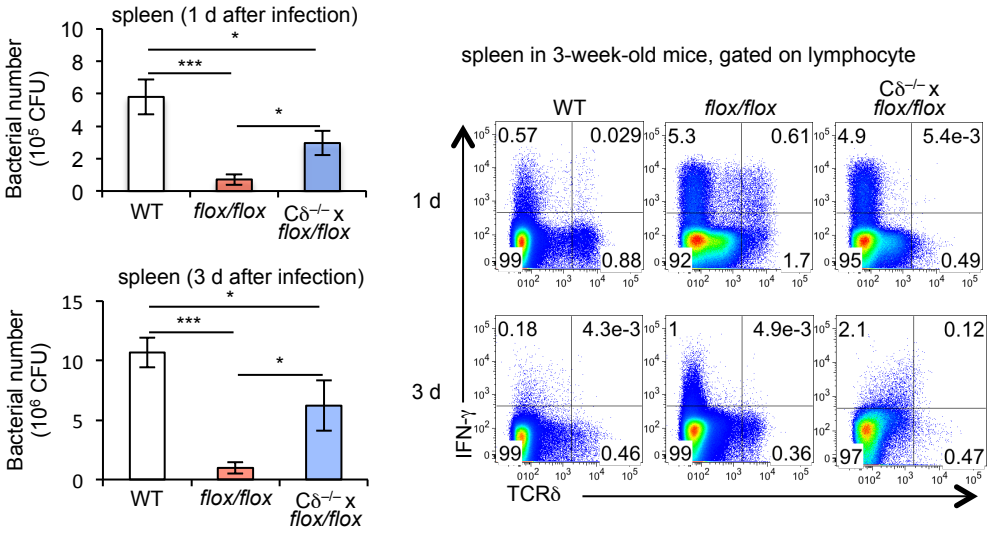

Supplemental Figure 6. Bcl11b-independent γδ T cells of spleen are involved in the host defense after *L. monocytogenes* infection (related to Figure 6)

Bar graphs show the means ± SD of bacterial number in the spleen from WT, *floxflox* and Cδ$^{-/-}$ × *flox/flox* mice on days 1 (upper panel) and 3 (under panel) after *L. monocytogenes* infection (n = 3). Representative dot plots are shown after gating on lymphocyte. Numbers in the quadrants indicate the percentage of expression of intracellular IFN-γ and TCRδ in lymphocytes of spleen from WT, *floxflox* and Cδ$^{-/-}$ × *flox/flox* mice on days 1 (upper panels) and 3 (under panels) after *L. monocytogenes* infection (n = 3). Significant differences are shown (*p<0.05, ***p<0.001: one way ANOVA/Tukey).

SUPPLEMENTAL EXPERIMENTAL PROCEDURES

Antibodies for Flow cytometry

Antibodies used in this study: PE-conjugated anti-CD3ε (145-2C11), PerCP-Cy5.5-conjugated anti-MHC class II (M5/114.15.2), APC-conjugated anti-IFNγ (XMG1.2), APC-Cy7-conjugated anti-CD3ε (145-2C11), PE-Cy7-conjugated anti-CD45.2 (104), V450-conjugated anti-CD4 (RM4–5), anti-CD8α (53–6.7), anti-IL-17A (TC11–18H10), and V500-conjugated anti-MHC class II (M5/114.15.2) mAbs were purchased from BD Biosciences (San Jose, CA, USA). FITC-conjugated anti-CD62L (MEL-14), Rat IgG2a κ isotype control (eBR2a) PE-conjugated anti-CD27 (LG.7F9), anti-CD44 (IM7), anti-CD62L (MEL-14), anti-CD117 (2B8), anti-CD122 (TM-b1), anti-CD127 (A7R34), anti-NKG2D (Cx5), Rat IgG2a κ isotype control (RTK2758), Rat IgG2a κ isotype control (RTK4530), Hamster IgG isotype control (HTK888), PerCP-Cy5.5-conjugated anti-IL-17A (ebio17B7), APC-conjugated anti-CD45.2 (104), PerCP-eFluor 710-conjugated anti-Granzyme B (NGZB) and biotin-conjugated anti-CD45.1 (A20) mAbs were all purchased from eBioscience (San Diego, CA, USA). FITC-conjugated anti-CD5 (53–7.3), anti-CD8β (YTS156.7.7), anti-CD44 (IM7), anti-CD244 (m2B4), anti-TCRβ (H57–597), anti-MHC class II (M5/114.15.2), anti-Vγ1 (2.11), PE-conjugated anti-CD5 (53–7.3), anti-CD8α (53–6.7), anti-NK1.1 (PK136), anti-MHC class II (M5/114.15.2), anti-Vγ1 (2.11), anti-Vγ4 (UC3–10A6), APC-conjugated anti-CD25 (PC61), anti-NKp46 (29A1.4), anti-TCRβ (H57–597), anti-TCRδ (GL3), anti-Vγ4 (UC3–10A6), Alexa Fluor 647-conjugated anti-CD3ε (17A2), anti-NK1.1 (PK136), Mouse IgG2a κ isotype control (MOPC-173) ,PE-Cy7-conjugated anti-CD4 (RM4–5), anti-TCRδ (GL3) mAbs and V421-conjugated anti-TCRδ (GL3) were purchased from BioLegend (San Diego, CA, USA). PE-conjugated anti-Vγ5 (536) mAb was purchased from Santa Cruz Biotechnology (Santa Cruz, CA, USA). FITC-conjugated anti-Ctip2 (25B6) and Rat IgG2a κ isotype control (RTK2758) mAb were purchased from Abcam (Cambridge, MA, USA)

Primers for RT-PCR

For analyzing the Bcl11b, Vγ, and Vδ repertoire, combinations of the following primers were used. Forward primers: β-actin, 5′-TGGAATCCTGTGGCATCCATGAAAC-3′; Bcl11b, 5′-TGTCCCAGAGGGAACTCATC-3′. Reverse primers: β-actin, 5′-TAAAACGCAGCTCAGTAACAGTCCG-3′; Bcl11b, 5′-CTTGTCCAGGACCTTGTCGT-3′. For the Vγ and Vδ repertoire analysis, combinations of following primers were used. Forward primers: Vγ 1/2, 5′-ACACAGCTATACATTGGTAC-3′; Vγ2, 5′-CGGCAAAAAACAAATCAACAG-3′; Vγ4, 5′-TGTCCTTGCAACCCCTACCC-3′; Vγ5, 5′-TGTCCTTGCAACCCCTACCC-3′; Vγ6, 5′-GGAATTCAAAAGAAAACATTGTCT-3′; Vγ7, 5′-AAGCTAGAGGGGTCCTCTGC-3′; Vδ1, 5′-ATTCAGAAGGCAACAATGAAAG-3′; Vδ2, 5′-AGTTCCCTGCAGATCCAAGC-3′; Vδ3, 5′-TTCCTGGCTATTGCCTCTGAC-3′; Vδ4, 5′-CCGCTTCTCTGTGAACTTCC-3′; Vδ5, 5′-CAGATCCTTCCAGTTCATCC-3′; Vδ6, 5′-TCAAGTCCATCAGCCTTGTC-3′; Vδ7, 5′-CGCAGAGCTGCAGTGTAACT-3′; Vδ8, 5′-AAGGAAGATGGACGATTCAC-3′; Reverse primers: Cγ 5′-CTTATGGAGATTTGTTTCAGC-3′; Cδ, 5′-CGAATTCCACAATCTTCT-3′.